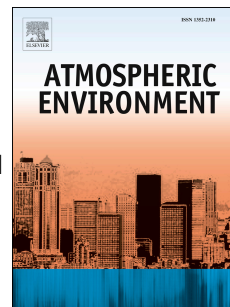


Accepted Manuscript



Evaluation of operational on-line-coupled regional air quality models over Europe and North America in the context of AQMEII phase 2. Part I: Ozone

Ulas Im, Roberto Bianconi, Efsio Solazzo, Ioannis Kioutsioukis, Alba Badia, Alessandra Balzarini, Rocío Baró, Roberto Bellasio, Dominik Brunner, Charles Chemel, Gabriele Curci, Johannes Flemming, Renate Forkel, Lea Giordano, Pedro Jiménez-Guerrero, Marcus Hirtl, Alma Hodzic, Luka Honzak, Oriol Jorba, Christoph Knote, Jeroen J.P. Kuenen, Paul A. Makar, Astrid Manders-Groot, Lucy Neal, Juan L. Pérez, Guido Pirovano, George Pouliot, Roberto San Jose, Nicholas Savage, Wolfram Schroder, Ranjeet S. Sokhi, Dimiter Syrakov, Alfreida Torian, Paolo Tuccella, Johannes Werhahn, Ralf Wolke, Khairunnisa Yahya, Rahela Zabkar, Yang Zhang, Junhua Zhang, Christian Hogrefe, Stefano Galmarini

PII: S1352-2310(14)00735-3

DOI: [10.1016/j.atmosenv.2014.09.042](https://doi.org/10.1016/j.atmosenv.2014.09.042)

Reference: AEA 13274

To appear in: *Atmospheric Environment*

Received Date: 27 May 2014

Revised Date: 12 September 2014

Accepted Date: 13 September 2014

Please cite this article as: Im, U., Bianconi, R., Solazzo, E., Kioutsioukis, I., Badia, A., Balzarini, A., Baró, R., Bellasio, R., Brunner, D., Chemel, C., Curci, G., Flemming, J., Forkel, R., Giordano, L., Jiménez-Guerrero, P., Hirtl, M., Hodzic, A., Honzak, L., Jorba, O., Knote, C., Kuenen, J.J.P., Makar, P.A., Manders-Groot, A., Neal, L., Pérez, J.L., Pirovano, G., Pouliot, G., San Jose, R., Savage, N., Schroder, W., Sokhi, R.S., Syrakov, D., Torian, A., Tuccella, P., Werhahn, J., Wolke, R., Yahya, K., Zabkar, R., Zhang, Y., Zhang, J., Hogrefe, C., Galmarini, S., Evaluation of operational on-line-coupled regional air quality models over Europe and North America in the context of AQMEII phase 2. Part I: Ozone, *Atmospheric Environment* (2014), doi: 10.1016/j.atmosenv.2014.09.042.

This is a PDF file of an unedited manuscript that has been accepted for publication. As a service to our customers we are providing this early version of the manuscript. The manuscript will undergo copyediting, typesetting, and review of the resulting proof before it is published in its final form. Please

note that during the production process errors may be discovered which could affect the content, and all legal disclaimers that apply to the journal pertain.

1 **Evaluation of operational on-line-coupled regional air quality models over**
2 **Europe and North America in the context of AQMEII phase 2. Part I:**
3 **Ozone**

4
5 Ulas Im^a, Roberto Bianconi^b, Efisio Solazzo^a, Ioannis Kioutsioukis^a, Alba Badia^c, Alessandra
6 Balzarini^d, Rocío Baró^e, Roberto Bellasio^b, Dominik Brunner^f, Charles Chemel^g, Gabriele
7 Curci^h, Johannes Flemmingⁱ, Renate Forkel^j, Lea Giordano^f, Pedro Jiménez-Guerrero^e,
8 Marcus Hirtl^k, Alma Hodzic^l, Luka Honzak^m, Oriol Jorba^c, Christoph Knote^l, Jeroen J.P.
9 Kuenenⁿ, Paul A. Makar^o, Astrid Manders-Grootⁿ, Lucy Neal^p, Juan L. Pérez^q, Guido
10 Pirovano^d, George Pouliot^r, Roberto San Jose^q, Nicholas Savage^p, Wolfram Schroder^s,
11 Ranjeet S. Sokhi^g, Dimiter Syrakov^t, Alfreida Torian^r, Paolo Tuccella^h, Johannes Werhahn^j,
12 Ralf Wolke^s, Khairunnisa Yahya^u, Rahela Zabkar^{m,v}, Yang Zhang^u, Junhua Zhang^o, Christian
13 Hogrefe^r, Stefano Galmarini^{a,*}

- 14
15 a. European Commission, Joint Research Centre, Institute for Environment and
16 Sustainability, Air and Climate Unit, Ispra (Italy).
17 b. Enviroware srl, Concorezzo (MB), Italy.
18 c. Earth Sciences Department, Barcelona Supercomputing Center (BSC-CNS),
19 Barcelona, Spain.
20 d. Ricerca sul Sistema Energetico (RSE SpA), Milano, Italy
21 e. University of Murcia, Department of Physics, Physics of the Earth. Campus de
22 Espinardo, Ed. CIOyN, 30100 Murcia, Spain.
23 f. Laboratory for Air Pollution and Environmental Technology, Empa, Dubendorf,
24 Switzerland.
25 g. Centre for Atmospheric & Instrumentation Research, University of Hertfordshire,
26 College Lane, Hatfield, AL10 9AB, UK.
27 h. Department of Physical and Chemical Sciences, Center of Excellence for the forecast
28 of Severe Weather (CETEMPS), University of L'Aquila, L'Aquila, Italy.
29 i. ECMWF, Shinfield Park, RG2 9AX Reading, United Kingdom.
30 j. Karlsruher Institut für Technologie (KIT), Institut für Meteorologie und
31 Klimaforschung, Atmosphärische Umweltforschung (IMK-IFU), Kreuzeckbahnstr. 19,
32 82467 Garmisch-Partenkirchen, Germany.
33 k. Section Environmental Meteorology, Division Customer Service, ZAMG -
34 Zentralanstalt für Meteorologie und Geodynamik, 1190 Wien, Austria.
35 l. National Center for Atmospheric Research, Boulder, CO, US.
36 m. Center of Excellence SPACE-SI, Ljubljana, Slovenia.
37 n. Netherlands Organization for Applied Scientific Research (TNO), Utrecht, The
38 Netherlands.
39 o. Air Quality Research Section, Atmospheric Science and Technology Directorate,
40 Environment Canada, 4905 Dufferin Street, Toronto, Ontario, Canada.
41 p. Met Office, FitzRoy Road, Exeter, EX1 3PB, United Kingdom.
42 q. Environmental Software and Modelling Group, Computer Science School - Technical
43 University of Madrid, Campus de Montegancedo - Boadilla del Monte-28660, Madrid,
44 Spain.

- 45 r. Emissions and Model Evaluation Branch, Atmospheric Modeling and Analysis
46 Division/NERL/ORD, Research Triangle Park, North Carolina, USA.
47 s. Leibniz Institute for Tropospheric Research, Permoserstr. 15, D-04318 Leipzig,
48 Germany.
49 t. National Institute of Meteorology and Hydrology, Bulgarian Academy of Sciences, 66
50 Tzarigradsko shaussee Blvd., Sofia 1784, Bulgaria.
51 u. Department of Marine, Earth and Atmospheric Sciences, North Carolina State
52 University, Raleigh, USA.
53 v. University of Ljubljana, Faculty of Mathematics and Physics, Ljubljana, Slovenia.

54
55 * Corresponding author: S. Galmarini (Stefano.galmarini@jrc.ec.europa.eu)
56

57 Highlights

- 58
59 • Sixteen modeling groups from EU and NA simulated O₃ for 2010 under AQMEII
60 phase 2
61 • A general model underestimation of surface O₃ over both continents up to 22%
62 • Models tend to over/under estimate surface O₃ in all regions during autumn/winter
63 • Boundary conditions influence O₃ predictions especially during winter and autumn
64 • Models tend to under-predict high O₃ values that are of concern for policy
65

66
67 Keywords: AQMEII, on-line coupled models, performance analysis, ozone, Europe, North
68 America
69

70 ABSTRACT

71
72 The second phase of the Air Quality Model Evaluation International Initiative (AQMEII)
73 brought together sixteen modeling groups from Europe and North America, running eight
74 operational online-coupled air quality models over Europe and North America on common
75 emissions and boundary conditions. With the advent of online-coupled models providing new
76 capability to quantify the effects of feedback processes, the main aim of this study is to
77 compare the response of coupled air quality models to simulate levels of O₃ over the two
78 continental regions. The simulated annual, seasonal, continental and sub-regional ozone
79 surface concentrations and vertical profiles for the year 2010 have been evaluated against a
80 large observational database from different measurement networks operating in Europe and
81 North America. Results show a general model underestimation of the annual surface ozone
82 levels over both continents reaching up to 18% over Europe and 22% over North America.
83 The observed temporal variations are successfully reproduced with correlation coefficients
84 larger than 0.8. Results clearly show that the simulated levels highly depend on the
85 meteorological and chemical configurations used in the models, even within the same
86 modeling system. The seasonal and sub-regional analyses show the models' tendency to
87 overestimate surface ozone in all regions during autumn and underestimate in winter.
88 Boundary conditions strongly influence ozone predictions especially during winter and
89 autumn, whereas during summer local production dominates over regional transport. Daily
90 maximum 8-hour averaged surface ozone levels below 50-60 $\mu\text{g m}^{-3}$ are overestimated by all
91 models over both continents while levels over 120-140 $\mu\text{g m}^{-3}$ are underestimated, suggesting
92 that models have a tendency to severely under-predict high O₃ values that are of concern for
93 air quality forecast and control policy applications.
94

95
96

1. Introduction

97 Tropospheric ozone (O_3) is an important secondary air pollutant produced by photochemical
98 oxidation of volatile organic compounds (VOC) and carbon monoxide (CO) in the presence of
99 nitrogen oxides (NO_x). It has implications on climate and health and therefore its levels are
100 subject to regulatory monitoring in Europe (EU) and North America (NA). The regulatory O_3
101 levels are still exceeded in a number of cities and are especially a concern in growing urban
102 areas (European Environmental Agency, 2013). Air quality models (AQMs) are valuable tools
103 to investigate the complex and dynamic interactions between meteorology and chemistry
104 leading to O_3 pollution episodes at multiple temporal and spatial scales. In the last decade,
105 AQM development started shifting from off-line-coupled models where the meteorological
106 forcing for chemistry was produced off-line by a separate meteorological model, to fully-
107 coupled online models, which are able to simulate the feedbacks between chemistry and
108 meteorology, taking the advantage of increased computational power (Zhang, 2008; Baklanov
109 et al., 2014). The use of on-line models for O_3 predictions is beneficial, as O_3 not only
110 depends on emissions and chemistry but also on regional transport, clouds, photolysis and
111 vertical mixing in the boundary layer, all of which can be more realistically represented in an
112 on-line model (Wong et al, 2012; Zhang et al, 2013). The impact of aerosols on the radiation,
113 and therefore temperatures and photolysis rates, can significantly impact the gas-phase
114 chemistry affecting O_3 and secondary aerosol formation (Kim et al., 2009, 2011). Thus,
115 simulating these feedbacks can lead to more realistic O_3 , NO_x and aerosol levels that are
116 relevant to policy applications. The wide use of regional AQMs for supporting policy,
117 abatement strategies and forecasting justifies the increased need for online models, which can
118 simulate feedback mechanisms, and especially account for the effect of aerosols on radiative
119 balance and photolysis (e.g. Hodzic et al., 2007).

120 The Air Quality Model Evaluation International Initiative (AQMEII) served to promote
121 policy-relevant research on regional air quality model evaluation across the atmospheric
122 modeling communities in Europe and North America through the exchange of information on
123 current practices and the identification of research priorities (Galmarini and Rao, 2011). As
124 part of this collaboration, standardized observations and model outputs were made available
125 through the ENSEMBLE system (<http://ensemble2.jrc.ec.europa.eu/public/>) that is hosted at
126 the Joint Research Centre (JRC). This web-interface allows temporal and spatial analyses of
127 individual models as well as their ensemble operators (Bianconi et al., 2004; Galmarini et al.,
128 2012). The first phase of AQMEII was focused on the evaluation of off-line coupled
129 atmospheric modelling systems against large sets of monitoring observations over Europe and
130 North America for the year 2006 (Solazzo et al., 2012a,b; Vautard et al., 2012; Solazzo et al.,
131 2013; Hogrefe et al., 2014). As summarized in Schere et al. (2012), the intercomparison
132 model results for O_3 suggested a strong influence of chemical boundary conditions for ozone,
133 whose bias extends far into the interior of the modelling domains, especially during winter
134 months. The observed variance as well as the daily ozone cycle was underestimated by the
135 majority of models. Night-time, overcast, and stable conditions led to poor model skill in
136 reproducing ozone mixing ratios over both continents. Stable atmospheric boundary layers
137 have been notoriously difficult to simulate in numerical weather prediction models (Holtslag

138 et al. 2013), but they are highly relevant in the context of air quality modeling. Due to the
139 high sensitivity of air pollutants to the representation of stable boundary layers, online
140 coupled modeling could be of great use to tackle this problem in the future.

141 The second phase of AQMEII extends this model assessment to on-line-coupled air quality
142 models. In this study, we analyze O₃ concentrations provided by eight on-line-coupled
143 models, which have been run by sixteen independent groups from Europe and North America
144 (while a companion study is devoted to the analyses of particulate matter, Im et al., 2014).
145 The models made use of the same input emissions and chemical boundary conditions, in an
146 effort to reduce the impact of uncertainties originating from these inputs to model results
147 among different groups. The goal of the study is to evaluate the performances of widely used
148 operational on-line coupled models in Europe and North America in simulating O₃ levels on a
149 sub-regional and seasonal basis employing an experimental set-up with common
150 anthropogenic emission and boundary conditions. The surface levels and vertical profiles
151 simulated by the individual models as well as their ensemble mean and median are compared
152 with the observational data provided by the ENSEMBLE system.

153

154 2. Materials and Methods

155 2.1. Participating models

156 In the context of AQMEII2, twelve modeling groups from EU and four modeling groups from
157 NA (Table 1) have applied their modeling systems to simulate hourly O₃ concentrations for
158 the year 2010 over the EU and NA continental scale domains (Fig.1). Among all participants,
159 seven groups from EU and two groups from NA applied the same model system (WRF-
160 CHEM), but with different settings such as different shortwave radiation schemes, gas-phase
161 chemical mechanisms and aerosol modules. The WRF-CHEM community applied a common
162 horizontal grid spacing of 23 km over Europe and 36 km over North America. Other
163 modeling groups applied different grid spacings, ranging from 12×12 km² to ~50×25 km² as
164 seen in Table 1. The simulations were conducted for continental-scale domains of Europe and
165 North America covering continental U.S., southern Canada and northern Mexico (Fig.1). To
166 facilitate the cross-comparison between models, the participating groups interpolated their
167 model output to a common grid with 0.25° resolution for both continents. Model values at
168 observation locations were extracted from the original model output files for comparison to
169 observations (described below).

170 2.2. Emissions and boundary conditions

171 For the EU domain, the recently updated anthropogenic emissions for the year 2009
172 (<http://www.gmes-atmosphere.eu/>; Kuenen et al., 2014; Pouliot et al., 2014) were applied by
173 all modelling groups and are based on the TNO-MACC-II (Netherlands Organization for
174 Applied Scientific Research, Monitoring Atmospheric Composition and Climate – Interim
175 Implementation) framework. Annual emissions of methane (CH₄), carbon monoxide (CO),
176 ammonia (NH₃), total non-methane volatile organic compounds (NMVOC), nitrogen oxides

177 (NO_x), particulate matter (PM₁₀, PM_{2.5}) and sulfur dioxide (SO₂) from ten activity sectors are
178 provided on a latitude/longitude grid of 1/8°×1/16° resolution. Emission inventories for the
179 NA domain were provided by US EPA and Environment Canada. The 2008 National
180 Emission Inventory (<http://www.epa.gov/ttn/chief/net/2008inventory.html>) and the 2008
181 Emission Modeling Platform (<http://www.epa.gov/ttn/chief/emch/index.html#2008>) with year
182 specific updates for 2006 and 2010 were used for the US portion of the modeling domain.
183 Canadian emissions were derived from the Canadian National Pollutant Release Inventory
184 (<http://www.ec.gc.ca/inrp-npri/>) and Air Pollutant Emissions Inventory
185 (<http://www.ec.gc.ca/inrp-npri/donnees-data/ap/index.cfm?lang=En>) values for the year
186 2006. These included updated spatial allocations for Canadian mobile emissions (Zhang et al,
187 2012) for the emissions of NH₃ (Makar et al, 2009), as well as other updates (Sassi et al,
188 2010). Mexican emissions were 2008 projected forward from a 1999 inventory (Wolf et al,
189 2009). Seven pollutants (CO, NO_x, NH₃, SO₂, PM₁₀, PM_{2.5}, and VOC) were used to develop
190 the model ready emission inventory. Further details and analyses of the anthropogenic
191 emissions used in both domains are provided in Pouliot et al. (2014). Annually-integrated
192 anthropogenic emissions for both domains are presented in Table 2 while the spatial
193 distribution of NO_x emissions for the EU and NA domains are depicted in Fig. 1. Table 2
194 shows that anthropogenic emissions per km² in EU are larger than those in NA, except for
195 PM₁₀. Particularly NO_x and NH₃ emissions in EU are more than a factor of two larger than
196 those in NA. Consistent temporal profiles (diurnal, day-of-week, seasonal) and vertical
197 distributions were also made available to maintain consistency among different groups.
198 NMVOC speciation factors were applied by all groups individually with a recommendation to
199 follow the NMVOC speciation profiles for EU by Visschedijk et al. (2007). The temporal
200 profiles for the EU anthropogenic emissions were provided from Schaap et al. (2005).
201 Chemical and temporal profiles for the EPA anthropogenic emissions were based on the
202 2007v5 modeling platform (<http://www.epa.gov/ttn/chief/emch/index.html#2008>).

203 Each modeling group used their own biogenic emission module as detailed in Table 1. The
204 majority of the models used the online MEGAN2 model (Model of Emissions of Gases and
205 Aerosols from Nature version 2; Guenther et al., 2006), two groups used the BEIS v3.14
206 model (Biogenic Emission Inventory System; Schewede et al., 2005) and one group (NL2)
207 used the Beltman et al. (2013) biogenic model. It should be noted that UK4 group used the
208 off-line simulated biogenic emissions provided by the Beltman et al. (2013) model. In
209 addition to the biogenic emissions algorithm used in the models, they may also differ in the
210 databases used for vegetation. Feedbacks may have a significant influence on biogenic
211 emissions; reductions in biogenic isoprene emissions of 20% were found with the introduction
212 of the aerosol indirect effect (Makar et al., 2014a). The biogenic isoprene emissions
213 calculated on-line by each group show a large variability as shown in Table 2 that may lead to
214 large differences in the simulated O₃ levels. Curci et al. (2009) showed that different biogenic
215 emission models may lead to a factor of 2 difference in domain-integrated isoprene emissions
216 over Europe while difference can be up to a factor of 5-6 locally. They estimated that these
217 differences on average may lead to an increase of 2.5 ppb in domain-mean surface O₃ levels
218 and up to 10-15 ppb locally in the Mediterranean. Hourly biomass burning emissions were
219 provided by the Finnish Meteorological Institute (FMI) fire assimilation system

220 (<http://is4fires.fmi.fi/>; Sofiev et al., 2009). More details on the fire emissions and their
221 uncertainties are discussed in Soares et al. (2014). The fire assimilation system provides only
222 data for total PM emissions. Emissions of other species (CO, NO, NH₃, SO₂, NMVOC) were
223 therefore deduced based on mass ratios relative to PM following Andreae and Merlet (2001).
224 NMVOC speciation followed Wiedinmeyer et al. (2011) combined with the mapping to
225 different chemical mechanisms proposed by Emmons et al. (2010). Note that the ES2a model
226 does not include biomass burning emissions and as it does not contain aerosols leading to a
227 lack of effect of aerosols on photolysis rate calculations and therefore producing
228 overestimated O₃ within the fire plumes (Badia and Jorba, 2014). Lightning NO_x is included
229 in the UK4 model (O'Connor et al., 2014) as well as in the global MACC model used for the
230 boundary conditions as described below.

231 3-D daily chemical boundary conditions were taken from the MACC re-analysis (Inness et al.,
232 2013). The MACC re-analysis (referred to as MACC hereafter) has been produced by
233 assimilating satellite observations of O₃, CO and NO₂ in the coupled system IFS-MOZART
234 (Flemming et al., 2009). As pointed out in Inness et al. (2013), the assimilation of satellite-
235 corrected O₃ greatly improved the ozone total columns and stratospheric profiles but did not
236 change significantly the surface levels because of the limited signal from this region in the
237 assimilated satellite observations. The chemical species available in the reanalysis included
238 O₃, NO_x, CO, CH₄, SO₂, NMVOCs, sea-salt, dust, organic matter, black carbon and sulfate.
239 NMVOC species had to be lumped or disaggregated according to the individual models'
240 chemical speciation and particulate matter size discretization.

241 2.3. Observations

242 Measurements of hourly surface O₃ concentrations for the year 2010 in EU were taken from
243 the European Monitoring and Evaluation Programme (EMEP; <http://www.emep.int/>) and the
244 European Air Quality Database (AirBase; <http://acm.eionet.europa.eu/databases/airbase/>) and
245 in NA from the Canadian National Atmospheric Chemistry (NAChem) Database and
246 Analysis Facility operated by Environment Canada (<http://www.ec.gc.ca/natchem/>) that
247 contains measurements from the Canadian National Air Pollution Surveillance Network
248 (<http://maps-cartes.ec.gc.ca/rnspa-naps/data.aspx>), the Canadian Air and Precipitation
249 Monitoring Network (<http://www.ec.gc.ca/natchem/>), the U.S. Clean Air Status and Trends
250 Network (<http://java.epa.gov/castnet/clearsession.do>), the U.S. Interagency Monitoring of
251 Protected Visual Environments Network (<http://views.cira.colostate.edu/web/DataWizard/>),
252 and the U.S. Environmental Protection Agency's Air Quality System database for U.S. air
253 quality data (<http://www.epa.gov/ttn/airs/airsaqs/detaildata/downloadaqsddata.htm>). In the
254 AQMEI2, rural, urban and suburban background stations were extracted from the EMEP and
255 AirBase networks. Given the coarse native grid resolutions used in different models (Table 1),
256 data from only rural background stations was used in the comparisons. Stations that have
257 more than 90% data availability have been selected for the comparisons. Regarding the whole
258 simulation domains, hourly surface O₃ observations were provided by 510 and 200 stations in
259 EU and NA, respectively. A geographical break-down into four sub-regions for each
260 continent has also been defined based on the climatological and source characteristics. The
261 geographical break-down of these stations overlaid with the annually-averaged anthropogenic

262 NO_x emissions is shown in Fig.1. Model evaluation statistics were computed for the four sub-
 263 regions separately. The European sub-region EU1 is characterized by north-western European
 264 sources with a transition climate between marine and continental and hosts 102 stations. Sub-
 265 region EU2 covers the north-eastern and central Europe sources as well as Germany with 277
 266 monitoring stations. Sub-regions EU3 and EU4 are characterized by a Mediterranean type
 267 climate. Sub-region 3 covers south-western sources including Italy (30 stations) while sub-
 268 region 4 covers the East Mediterranean with 101 stations. The North American sub-region 1
 269 (NA1) covers the western U.S. and south western Canada with 80 stations. It includes large
 270 emission sources along the coast as well as polluted hot spots like Los Angeles that are
 271 characterized by poor air quality. NA2 consists of U.S. plains and covers 36 monitoring
 272 stations and is characterized by a continental and humid climate. NA3 consists of north
 273 eastern NA and south central Canada and is characterized by the largest emissions in North
 274 America and contains 60 monitoring stations. Finally NA4 covers the south eastern part of
 275 U.S., consisting of 24 monitoring stations.

276 To evaluate the capability of the modeling systems to simulate the tropospheric distribution of
 277 O₃ concentrations, comparisons against O₃ soundings provided by the World Ozone and
 278 Ultraviolet Radiation Data Centre (WOUDC: <http://www.woudc.org/>) have been carried out.
 279 Ozone concentration data from nine stations in EU and six stations in NA have been used for
 280 the comparisons. For an optimal comparison with observations, model profiles were
 281 computed by averaging only over the available observation hours. The participants were
 282 required to provide their data at fixed heights up to 18 km above the ground in order to be
 283 comparable. However, due to the coarse vertical resolution of some models in the upper
 284 troposphere and not simulating the stratospheric chemistry, the analyses are performed only
 285 for the first 9 km above ground.

286 2.4. Statistical analyses

287 To score the individual model performances as well as those of the ensemble mean and
 288 median, the following statistical parameters have been calculated: Pearson's correlation
 289 coefficient (*PCC*: Eq.1), root mean square error (*RMSE*: Eq.2); normalized mean standard
 290 error (*NMSE*: Eq.3) and normalized mean bias (*NMB*: Eq.4).

$$291 \quad PCC = \left[\frac{\frac{1}{N} \sum_{i=1}^N (O_i - \bar{O})(P_i - \bar{P})}{\sigma_O \sigma_P} \right] \quad (\text{Eq. 1})$$

$$292 \quad RMSE = \sqrt{\frac{1}{N} \sum_{i=1}^N (P_i - O_i)^2} \quad (\text{Eq. 2})$$

$$293 \quad NMSE = \frac{\sum_{i=1}^N (P_i - O_i)^2}{N \times \bar{P} \times \bar{O}} \times 100 \quad (\text{Eq. 3})$$

$$294 \quad NMB = \frac{\sum_{i=1}^N (P_i - O_i)}{\sum_{i=1}^N O_i} \times 100 \quad (Eq. 4)$$

295 where P and O denote model predictions and observations, respectively. The PCC is a
 296 measure of associativity and allows gauging whether trends are captured, and it is not
 297 sensitive to bias; $RMSE$ is a measure of accuracy and, because it is squared, is sensitive to
 298 large departures. $NMSE$ and NMB are normalised operators, useful for comparing scores
 299 coming from time series of different lengths, as those produced over different areas and/or
 300 with different time span. The comparison is performed individually for the two domains and
 301 their sub-regions for the whole year of 2010 and on a seasonal basis, in order to identify
 302 which regions and/or seasons lead to systematic errors.

303

304 3. Results and Discussion

305 3.1. Surface ozone analyses

306 Observed and simulated diurnal cycles of surface O_3 concentrations averaged over the whole
 307 simulation period (2010) are shown in Fig. 2a,d for EU and NA, respectively. Models are
 308 labelled by the ID of the respective modeling group, with each ID corresponding to a member
 309 of the overall model ensemble. In the same figures, the MACC IFS-MOZART global model
 310 (MACC) and the ensemble mean and median are also shown. Note that the MACC model is
 311 not considered in the ensemble calculations.

312 3.1.1. Europe

313 Most models capture reasonably well the shape of the annual diurnal cycle over Europe as
 314 seen in Fig.2. The temporal variations on all time scales were captured successfully as seen in
 315 Table 3 ($PCC > 0.80$), although the predicted O_3 levels are generally underestimated by up to
 316 18%. Only one group (UK4) slightly overestimates the yearly-averaged observed surface O_3
 317 levels by 2% while the other groups have underestimations up to 18%. The largest
 318 underestimations are calculated for IT2 (by 16%) and CH1 (by 18%) groups. Other groups
 319 have mean normalized biases within the $\pm 5\%$ to 15% range suggested by Russell and Dennis
 320 (2000). Fig.2a shows that the underestimations generally occur both during day and night
 321 hours, which is expected to some extent given the coarse horizontal resolution (Qian et al.,
 322 2010). The exceptions are AT1, DE4, SI1 and UK4 that overestimate the night time levels.
 323 The MACC model underestimates the nighttime levels as also reported in Innes et al. (2013).
 324 Overestimation of nighttime O_3 levels can be due to the overestimation of NO_2 concentrations
 325 under low- NO_x conditions leading to overestimated O_3 concentrations (e.g. DE4). Fig.2a
 326 shows that the underestimations generally occur both during day and night hours, which is
 327 expected to some extent given the coarse horizontal resolution (Qian et al., 2010). The
 328 exceptions are AT1, DE3, DE4, SI1, and UK4 that overestimate the night time levels. The
 329 MACC model underestimates the nighttime levels as also reported in Innes et al. (2013). The

330 small overestimation of nighttime O_3 levels for AT1 and SI1 can be attributed to the
331 underestimation of nocturnal ozone titration in urban areas with high NO_x emissions for the
332 QSSA solver that was applied for these simulations. For DE4, where a modified version of
333 this solver (Forkel et al., 2014) has been applied, the overestimation of nighttime ozone can
334 be attributed to a general overestimation of NO_2 concentrations under low- NO_x conditions.
335 This is also the case for the DE3 model during the nighttime, where this overestimation is
336 probably related to difficulties of the meteorological model to simulate nighttime vertical
337 mixing accurately and, furthermore, to comparatively small dry deposition fluxes for O_3
338 simulated by the model (see Table 3). It should be noted that the ES2a model does not include
339 anthropogenic aerosols and secondary aerosol formation and neither aqueous chemistry,
340 leading to a more oxidized atmosphere. Furthermore, the heterogeneous formation of HNO_3
341 through N_2O_5 hydrolysis, which is an important sink of NO_2 during night, is not considered in
342 ES2a (Badia and Jorba, 2014). As a consequence, the ES2a model overestimated the annual
343 domain-mean NO_2 levels by 15% while the rest of the models underestimate NO_2 by 9% to
344 45%. The overestimation of surface O_3 levels by the ES2a model can also partly be due to the
345 coarser vertical resolution of its first layer (45 m) compared to other models (Table 1). The
346 general underestimation may be partly attributed to biases in meteorological variables,
347 including an overestimation of surface wind speeds by all models by up to 60% and a general
348 slight underestimation of surface temperatures by less than 1 K (Brunner et al., 2014). Such a
349 small temperature bias, however, will affect ozone levels by no more than a few ppb (Sillman
350 and Samson, 1995). A common feature of all groups is that the daily maximum is simulated
351 earlier than the observed maximum. Differences in O_3 predictions between the WRF-CHEM
352 models suggest that the choice of the chemical mechanism plays an important role in the
353 model performance. WRF-CHEM runs using RADM chemical mechanism (AT1, ES1 and
354 SI1) produced higher concentrations than runs using RACM (IT2) and CBMZ (ES3 and IT1)
355 mechanisms (Baro et al., 2014). These differences may partly be attributed to VOC emission
356 preprocessing. WRF-CHEM is designed to ingest VOC emissions for RADM2 and then, in
357 case of other mechanisms, the emissions are chemically specified to the final scheme,
358 possibly leading to a degradation of the reactivity in the VOC mixture. There are also
359 differences in the microphysics schemes among the different WRF-CHEM configurations
360 used, leading to different cloudiness and therefore to different temperature and radiation
361 acting on the O_3 production (Brunner et al., 2014; Baro et al., 2014). Makar et al. (2014a) and
362 Wang et al. (2014) found that models including the simulation of indirect effects tended to
363 have lower O_3 concentrations during the summer production period than those with the direct
364 effect only, or those with no feedbacks. This is due to the reduction of NO_2 mixing ratios
365 during daytime and near-surface temperatures, resulting from the reduction of solar radiation
366 (Wang et al., 2014). Dry deposition of O_3 is also investigated for the models that provided
367 deposition data (CH1, DE3, DE4, ES1, ES2a, ES3, IT2, NL2 and SI1) in order to explain the
368 differences in simulated O_3 levels among the models (Table 3). The results show a negative
369 relation between underestimation and dry deposition; i.e. the underestimation increases with
370 decreasing deposition, suggesting that other terms aside from deposition were controlling the
371 O_3 concentrations (chemistry, vertical diffusion etc.).

372 The model performances are also assessed against the observed variability in box-and-whisker
373 plots of Fig.2b and e. The plot shows the frequency distribution of observed and simulated
374 surface O₃ mixing ratios. The spread of the data in the European case is largest in CH1, ES2a
375 and UK4 (Fig. 2b). The majority of other models show a much lower spread, which also tends
376 to be lower than the observed spread. Data from MACC are associated with a larger spread
377 compared to the observations in both domains, suggesting a better representation of local
378 processes by regional models as well as an indication of an exaggerated seasonal cycle
379 simulated by the MACC model. The larger spread in some models as compared to others is
380 partially related to the amplitude of the diurnal ozone cycle, which tends to be larger in
381 models simulating a more stable and shallow nocturnal PBL such as the global MACC model
382 (Innes et al., 2013). A larger amplitude may also be expected for models with a higher vertical
383 resolution. The *NMB* vs *NMSE* plot (also known as the soccer diagram) for EU (Fig. 2c)
384 shows that the models have mean biases below 30% and mostly below 15%. The geographical
385 analyses for the EU domain presented in Fig.3 show that for the majority of models, the
386 underestimation is mainly originating from sub-region EU2 (north Eastern Europe) while in
387 sub-region EU4 (East Mediterranean), most models overestimate the observed mean. The
388 underestimation, particularly in EU1 and EU2 could be partly due to the chemical boundary
389 conditions (Fig.3) as discussed in more detail in Sect. 3.3.

390 3.1.2. North America

391 The hourly O₃ temporal variability over the whole simulation period is also well captured
392 (*PCC*>0.78) by all groups for the NA domain (Table 3). The CA2f model overestimates the
393 nighttime surface O₃ concentrations and underestimates the daytime levels with a slight
394 overall overestimation of 2% while other groups underestimate the nighttime levels (Fig.2d).
395 *NMSE* values are below 10% for all the groups while *NMB* values are within ±15% except for
396 the US8 model, which underestimates the surface O₃ levels by 22%. The box plots for the NA
397 case (Fig. 2e) shows that the MACC model has the highest variability while CA2f is
398 characterized with the smallest spread. Larger biases in US7 and US8 can also be partly
399 attributed to their coarser resolution (36 km) compared to other NA models (Table 1). In the
400 NA case, according to the soccer diagrams (Fig. 2f), all groups and sub-regions are
401 characterized with biases lower than 25% except for US8. The geographical break down
402 presented in Fig.4 shows that the US8 model underestimates in all sub-regions. The MACC
403 model also shows a general underestimation in all sub-regions except for NA4. Regarding the
404 dry deposition of O₃ (Table 3), the results suggest that the large underestimation by US8 can
405 be partly due to the relatively large O₃ dry deposition simulated by the model, acting as a
406 significant sink. As analyzed in Yahya et al. (2014a,b) and Wang et al. (2014), other factors
407 that contribute to underpredictions of O₃ by the US8 model include large underpredictions of
408 afternoon temperatures, low MACC boundary conditions of O₃, the overpredictions of the
409 NO_x titration effects on O₃ during nighttime, possible underestimates in biogenic VOCs and
410 wildfire emissions, and the inclusion of aerosol indirect effects. The lower spread in CA2f
411 seems to be due to overpredicting the lower end of the O₃ range compared to the observations,
412 in regions NA3 and NA4.

413 3.2. Seasonal vs. geographical surface ozone variations

414 3.2.1. Europe

415 Inter-seasonal variations of surface O₃ concentrations are analyzed for each sub-region in
416 order to understand how the model bias varies depending on the region and season. The
417 results for the EU domain are depicted in Fig. 5. The temporal variability in Europe is better
418 captured in all models in summer and autumn ($PCC=0.8-0.9$) than in winter and spring
419 ($PCC=0.6-0.8$). There is a systematic overestimation of the observed concentrations in
420 autumn by up to 35%, particularly by the DE4 model. In winter (Fig. 5a), O₃ mixing ratios in
421 EU2 are underestimated by more than 50% by three groups (CH1, ES2a and UK4), which
422 also underestimate systematically in other sub-regions, probably due to the bias from the
423 boundary conditions from the MACC model. The MACC model underestimates by largest
424 during winter (by 8% to 55%) and overestimates by largest in autumn (by 8% to 25%).
425 Regarding EU1, all groups are within the 30% bias range. Spring and summer O₃ mixing
426 ratios (Fig. 5b,c) in all EU sub-regions are similarly reproduced by all groups, with error
427 below 30%. In autumn, the majority of the models are biased high. In northern Europe (EU1
428 and EU2), the majority of the models underestimate O₃ levels in all seasons with the DE4,
429 UK4, and ES2a models overestimating during summer. There is a general overestimation in
430 autumn in the EU1 sub-region by all models except for CH1 and IT2. The models NL2, DE4,
431 UK4 and ES2a overestimate the summertime O₃ levels in southern Europe. The East
432 Mediterranean region (EU4) is characterized by overestimated O₃ levels, in particular during
433 autumn. The results show that the largest underestimations were calculated for the EU2
434 region, which is characterized with large anthropogenic emissions in the Eastern Europe that
435 may lead to overestimated O₃-titration by NO_x.

436 3.2.2. North America

437 Inter-seasonal and geographical variations of the models performances in NA are presented in
438 Fig.6. US8 underestimates the observations in all seasons and in particular in winter and
439 spring, and much larger compared to other models. In sub-region NA1, US6 overestimates by
440 up to 9% while US8 underestimates by up to 22% in all seasons. CA2f slightly overestimates
441 the winter and autumn O₃ levels by 3% and 5%, respectively. In the sub-regions NA2 and
442 NA3, there is a general underestimation of all O₃ in winter and spring and a general
443 overestimation in summer and autumn except for the US8 model. The winter and spring
444 underestimates may be the result of underpredictions of afternoon temperatures and excessive
445 O₃ titration by NO_x as NA3 can be characterized by the largest emission sources in NA. In
446 NA4, summertime O₃ levels are overestimated by all models including the US8 model.
447 Slightly lower correlation coefficients ($PCC=0.7-0.9$) are calculated for winter in NA while
448 other seasons are simulated with PCC values of $\sim 0.8-0.9$, with slightly lower PCC values
449 calculated for US7 (not shown).

450 3.3. Influence of chemical boundary conditions

451 The influence of the chemical boundary conditions on the simulated surface O₃ levels has also
452 been investigated on a seasonal basis. The analysis is carried out for the EU2 (north Eastern
453 Europe) sub-region for Europe assuming that it is the least affected by the dominant westerly
454 transport and having large anthropogenic emissions, suggesting that O₃ levels are more

455 strongly controlled by local processes than regional transport, compared to the other sub-
456 regions. Following the same rationale, sub-region NA3 was selected for the NA domain. The
457 results presented in Fig.7a show that in winter, all models underestimate O₃ levels along with
458 the MACC model that provides the boundary conditions suggesting that large scale
459 circulation and chemistry dominates over the local O₃ production. In spring and in summer
460 (Fig.7b,c), the regional production is more important than transport due to increased
461 photochemical activity. In autumn (Fig.7d), transport becomes more effective over local
462 production. The MACC model slightly overestimates the summer levels (*NMB*=1%), and
463 slightly underestimates the autumn levels (*NMB*=-5%) while it underestimates the winter and
464 spring levels 55% and 21%, possibly leading to the systematic overestimation of the regional
465 models in autumn. The impact of large-scale transport over NA is less pronounced compared
466 to Europe (Fig.8). The impact is the smallest during summer when photochemical production
467 is the largest (Fig.8c). At the same time, it is interesting to note that the MACC results in the
468 winter for NA1 are the lowest of the models shown in Fig.8a, with a deficit of 8 ppb relative
469 to the observations at 0 LST. The implication is that local chemistry, physics, model
470 resolution and/or emissions relative to the global model all account for an increase in the
471 winter O₃ levels for region NA1 of 8 ppb (28.5%), and these local effects are captured by the
472 suite of regional models. This may be compared to findings from the HTAP experiment,
473 which suggest a 20% reduction in emissions in Europe, South Asia and East Asia would result
474 in a 0.9 ppb reduction in O₃ in North America (Reidmiller et al, 2009). Here, simulated O₃
475 levels seem to be much more sensitive to the local O₃ chemistry than to the boundary
476 conditions associated with long-range transport (winter being the dominant season for long-
477 range transport effects). Over both continents, the nighttime differences in all seasons are
478 particularly large, with the MACC model largely underestimating the nighttime O₃. Similar
479 results were reported by Solazzo et al. (2012 and 2013a) for the first phase of the AQMEII
480 project. A more detailed analysis of the influence of the MACC boundary conditions on a
481 range of simulated species is presented in Giordano et al. (2014).

482 3.4. Multi-model mean and median

483 The combination of concentrations simulated by several models can enhance the skill when
484 compared to those from individual models (Galmarini et al., 2004a,b), which has also been
485 demonstrated by Solazzo et al. (2012) in the first phase of the AQMEII project. In the present
486 study, we provide simple multi-model mean and median analyses. Therefore, the calculated
487 multi-model mean and median presented in Table 3-5 and in Fig.2-11 can only provide a
488 basic distribution of all models with respect to the observations and should not be treated as
489 multi-model ensemble analyses as they represent the bias originating from each individual
490 model. As shown in Solazzo et al. (2012, 2013b) and Kioutsioukis and Galmarini (2014),
491 introducing correlated biases into ensembles and analysis of the redundancy of the datasets is
492 essential. As detailed multi-model ensemble analysis is not the scope of this paper, further
493 analyses have been performed by Kioutsioukis et al. (2014) for the EU case using the multi-
494 model data presented in the present paper.

495 3.5. Regulatory analysis based on 8-hour maximum surface O₃

496 Observed and simulated daily maximum 8-hour averaged surface O₃ levels during the O₃
497 season (May-September), which is a regulatory metric used in EU and NA, are compared in
498 order to understand how the model biases vary with O₃ levels. The results are shown in Fig.9
499 (note that in Fig.9, observed concentrations are presented by /10). Over EU, all models
500 overestimate O₃ concentrations below 50 µg m⁻³ by ~40% to ~80% while they underestimate
501 values above 140 µg m⁻³ except for the UK4 model that overestimates the levels above 160 µg
502 m⁻³. Most models follow the MACC model up to a concentration of 200 µg m⁻³ with
503 increasing variability towards higher concentrations. NL2 and UK4 models overestimate the
504 230-240 µg m⁻³ concentration bin where the spread is also largest among other models. The
505 UK4 model defines the upper boundary while IT2 defines the lower boundary of the envelope
506 until 100 µg m⁻³ while above that, the highest differences are calculated for IT1. The CH1
507 model, which together with the IT2 model showed the largest negative biases in annual mean
508 values, is more consistent with other models when considering 8-hour maximum values.
509 Above a concentration of 70 µg m⁻³, ES2a, NL2 and UK4 models are associated with positive
510 deviations from the MACC model while other models are below the MACC-simulated levels.
511 Results show that depending on the station, there are underestimations by up to >200 µg m⁻³.

512 Over NA (Fig.9b), the biases are lower compared to EU. Note that for NA the values are
513 reported in volume mixing ratios (ppb) rather than concentrations (µg/m³). The surface O₃
514 levels below 30 ppb are overestimated by all models by ~15-25% and levels above 60 ppb are
515 underestimated by all models by up to ~80%. The largest biases are calculated for US8 except
516 for the 120-130 ppb bin where US7 has the largest bias. US8 has the smallest bias below 50
517 ppb. The results show that models have a tendency to severely underpredict high O₃ values
518 which are of concern for air quality forecast and control policy applications. Further
519 improvement of model treatments (e.g., gas-phase chemistry, O₃ dry deposition and processes
520 affecting afternoon temperature predictions) and inputs (e.g., boundary conditions, biogenic
521 VOCs and wildfire emissions) as well as a better understanding of interplays among on-line-
522 coupled atmospheric processes (e.g., the impact of aerosol indirect effects on O₃ formation)
523 are urgently needed.

524 3.6. Vertical ozone profiles

525 The model results from each group as well as the ensemble mean and median are compared
526 with O₃ soundings obtained from WOUDC for the EU and NA domains up to 9 km height
527 above the ground. Figs.10 and 11 show the observed and simulated vertical O₃ levels at fixed
528 heights over the EU and NA domains, respectively while Tables 4 and 5 present the
529 normalized mean bias (*NMB*) for all the models and ensemble mean and median. On average,
530 most models underestimate the observed vertical profiles by up to 22% over EU. The DE4
531 model generally has smaller biases compared to other groups except for the station STN156
532 where it overestimates by ~12% (Fig.10). The ensemble mean/median improves the results
533 compared to the majority of the models depending on the station. The ensemble mean results
534 in smaller biases compared to the median. Over NA (Fig.11), the CA2f model underestimates
535 the vertical O₃ levels at all stations by 10-17% (Table 5). US6 and US7 have the smallest
536 biases in most stations but with overestimations of 14% and 5%, respectively, at STN457. The

537 US8 model underestimates at all stations by 4-15% but overestimates at STN457 by 2%. The
538 ensemble mean and median lead to improved results compared to CA2f at all stations above
539 ~1000-2000 m and to US8 at STN107 and STN456 below 2000-3000 m. Over Europe, among
540 others, STN318 station (Valentia Observatory, Ireland) can be considered as a site that is
541 largely impacted by long-range transport and is associated with the largest underestimation
542 ($NMB = -11\%$) by the MACC model (not shown), suggesting that boundary conditions can
543 partly contribute to the underestimated vertical profiles by a majority of the models. Results
544 also show that the tropospheric biases in the MACC model (Fig.10,11) are less pronounced
545 than the surface bias as also shown by Inness et al. (2013).

546

547 4. Summary and Conclusions

548 An operational evaluation of simulated ozone (O_3) levels over Europe (EU) and North
549 America (NA) in 2010 using eight different on-line-coupled air quality models from sixteen
550 groups has been conducted in the context of the AQMEII project. Seven groups from EU and
551 two groups from NA applied the WRF-CHEM model, but with different settings.
552 Anthropogenic emissions and chemical boundary conditions were prescribed while biogenic
553 emissions were calculated online by each individual group. All groups interpolated their
554 model output to a common output grid and a common set of receptor locations and uploaded
555 the data to the ENSEMBLE system. The results are evaluated against surface and sounding
556 observations, which are provided by operational over EU and NA, at continental and sub-
557 regional levels on annual and seasonal basis.

558 All models capture, reasonably well, the shape of the domain-averaged annual diurnal cycle
559 of O_3 over both domains, while the sub-regional temporal variability are simulated from
560 moderate to good depending on the season and the sub-region that the particular model is
561 configured for. There is a general underestimation of the annual surface O_3 by up to 18% and
562 22% over EU and NA, respectively. Differences in performance among models can be
563 attributed partly to the chemical mechanism used in the models, partly to VOC preprocessing
564 and different biogenic emissions, and partly to the differences in the microphysics, leading to
565 different cloudiness and therefore to different photolysis, temperature and radiation acting on
566 the O_3 production. The sub-regional analyses highlight the influence of the anthropogenic
567 emissions while the seasonal analyses show a strong tendency to overestimate the autumn
568 surface levels. The temporal variation and magnitudes are much better captured during
569 summer compared to other seasons. The winter and spring underestimations may be resulting
570 from underprediction of afternoon temperatures, excessive O_3 titration by too much NO_x as
571 well as biases from the chemical boundary conditions. Boundary condition analyses show that
572 wintertime levels are mostly driven by transport rather than local production due to limited
573 photochemistry. The global MACC model providing the boundary conditions to the regional
574 models largely underestimate the surface ozone levels particularly in winter, leading to a
575 negative bias in the regional model simulations, while in most sub-regions, it largely
576 overestimates the autumn O_3 levels in winter, leading to the systematic overestimations of
577 surface autumn O_3 levels by the regional models. The inclusion of aerosol indirect effects in

578 some online-coupled models also contributes in part to the underpredictions of O₃ mixing
579 ratios. On average, most models underestimate the observed vertical profiles by up to 22%
580 over EU and up to 17% over NA.

581 Comparison of observed and simulated daily maximum 8-hour averaged surface O₃ levels
582 during the O₃ season (May-September), which is a regulatory metric used in EU and NA,
583 show that over Europe, O₃ concentrations below 50 µg m⁻³ are overestimated by up to 80%
584 while levels above 140 µg m⁻³ are underestimated. Over NA the surface O₃ levels below 30
585 ppb are overestimated by all models by up to 25% and levels above 60 ppb are
586 underestimated by all models by up to 80%. This has implications for air quality forecast and
587 policy applications.

588 Overall, the results show a slight improvement in the surface ozone level predictions over EU
589 by the models that participated in the second phase of AQMEII compared to those that
590 participated in the first phase. The *NMB* calculated for the whole domain and simulation
591 period in the first phase ranged from -24% to 9% while in this second phase, the *NMB* range
592 was calculated to be -18% to 2%. On the other hand over NA, there is a significant change
593 between the two phases of the project: the overestimation of 3% to 22% in the first phase
594 shifted to a *NMB* range of -22% to 3%. These results, however, should not be considered as
595 solely the difference between on-line and off-line models as different simulation years,
596 different emissions, different sets of models, particularly for the NA case, and different
597 boundary condition data should be taken into account. Additionally, as the results presented in
598 this paper are temporally and spatially averaged, cases where feedback mechanisms are of
599 importance must be further studied and evaluated.

600

601 Acknowledgements

602 We gratefully acknowledge the contribution of various groups to the second air Quality
603 Model Evaluation international Initiative (AQMEII) activity: U.S. EPA, Environment Canada,
604 Mexican Secretariat of the Environment and Natural Resources (Secretaría de Medio
605 Ambiente y Recursos Naturales-SEMARNAT) and National Institute of Ecology (Instituto
606 Nacional de Ecología-INE) (North American national emissions inventories); U.S. EPA
607 (North American emissions processing); TNO (European emissions processing);
608 ECMWF/MACC project & Météo-France/CNRM-GAME (Chemical boundary conditions).
609 Ambient North American concentration measurements were extracted from Environment
610 Canada's National Atmospheric Chemistry Database (NAtChem) PM database and provided
611 by several U.S. and Canadian agencies (AQS, CAPMoN, CASTNet, IMPROVE, NAPS,
612 SEARCH and STN networks); North American precipitation-chemistry measurements were
613 extracted from NAtChem's precipitation-chemistry data base and were provided by several
614 U.S. and Canadian agencies (CAPMoN, NADP, NBPMN, NSPSN, and REPQ networks); the
615 WMO World Ozone and Ultraviolet Data Centre (WOUDC) and its data-contributing
616 agencies provided North American and European ozonesonde profiles; NASA's AEROSOL
617 RObotic NETwork (AeroNet) and its data-contributing agencies provided North American

618 and European AOD measurements; the MOZAIC Data Centre and its contributing airlines
619 provided North American and European aircraft takeoff and landing vertical profiles; for
620 European air quality data the following data centers were used: EMEP European Environment
621 Agency/European Topic Center on Air and Climate Change/AirBase provided European air-
622 and precipitation-chemistry data. The Finish Meteorological Institute is acknowledged for
623 providing biomass burning emission data for Europe. Data from meteorological station
624 monitoring networks were provided by NOAA and Environment Canada (for the US and
625 Canadian meteorological network data) and the National Center for Atmospheric Research
626 (NCAR) data support section. Joint Research Center Ispra/Institute for Environment and
627 Sustainability provided its ENSEMBLE system for model output harmonization and analyses
628 and evaluation. The co-ordination and support of the European contribution through COST
629 Action ES1004 EuMetChem is gratefully acknowledged. The views expressed here are those
630 of the authors and do not necessarily reflect the views and policies of the U.S. Environmental
631 Protection Agency (EPA) or any other organization participating in the AQMEII project. This
632 paper has been subjected to EPA review and approved for publication. C. Knote was
633 supported by the DOE grant DE-SC0006711. The UPM authors thankfully acknowledge the
634 computer resources, technical expertise and assistance provided by the Centro de
635 Supercomputación y Visualización de Madrid (CESVIMA) and the Spanish Supercomputing
636 Network (BSC). G. Curci and P. Tuccella were supported by the Italian Space Agency (ASI)
637 in the frame of PRIMES project (contract n.I/017/11/0). The Centre of Excellence for Space
638 Sciences and Technologies SPACE-SI is an operation partly financed by the European Union,
639 European Regional Development Fund and Republic of Slovenia, Ministry of Higher
640 Education, Science, Sport and Culture. Y. Zhang acknowledges funding support from the
641 NSF Earth System Program (AGS-1049200) and high-performance computing support from
642 Yellowstone by NCAR's Computational and Information Systems Laboratory, sponsored by
643 the National Science Foundation and Stampede, provided as an Extreme Science and
644 Engineering Discovery Environment (XSEDE) digital service by the Texas Advanced
645 Computing Center (TACC). The technical assistance of Bert van Ulft (KNMI) and Arjo
646 Segers (TNO) in producing the results of the RACMO2-LOTOS-EUROS system is gratefully
647 acknowledged. L. Giordano was supported by the Swiss SERI COST project C11.0144. The
648 UMU group acknowledges the funding from the project CGL2013-48491-R, Spanish
649 Ministry of Economy and Competitiveness.

650

651 REFERENCES

- 652 Andreae, M.O., Merlet, P., 2001. Emission of trace gases and aerosols from biomass burning.
653 *Global Biogeochemical Cycles*, 15, 4, 955-966.
- 654
- 655 Badia, A. and Jorba, O., 2014. Gas-phase evaluation of the online NMMB/BSC-CTM model
656 over Europe for 2010 in the framework of the AQMEII-Phase2 project. *Atmospheric*
657 *Environment*, <http://dx.doi.org/10.1016/j.atmosenv.2014.05.055>, In Press.
- 658
- 659 Baklanov, A., Schlünzen, K., Suppan, P., Baldasano, J., Brunner, D., Aksoyoglu, S.,
660 Carmichael, G., Douros, J., Flemming, J., Forkel, R., Galmarini, S., Gauss, M., Grell, G.,

- 661 Hirtl, M., Joffre, S., Jorba, O., Kaas, E., Kaasik, M., Kallos, G., Kong, X., Korsholm, U.,
662 Kurganskiy, A., Kushta, J., Lohmann, U., Mahura, A., Manders-Groot, A., Maurizi, A.,
663 Moussiopoulos, N., Rao, S. T., Savage, N., Seigneur, C., Sokhi, R. S., Solazzo, E.,
664 Solomos, S., Sørensen, B., Tsegas, G., Vignati, E., Vogel, B., Zhang, Y., 2014. Online
665 coupled regional meteorology chemistry models in Europe: current status and prospects.
666 *Atmospheric Chemistry and Physics*, 14, 317-398.
- 667
668 Baró, R., Jiménez-Guerrero, P., Balzarini, A., Curci, G., Forkel, R., Hirtl, M., Honzak, L.,
669 Im, U., Lorenz, C., Pérez, J.L., Pirovano, G., San José, R., Tuccella, P., Werhahn, J., Zabkar,
670 R., 2014. Sensitivity analysis of the microphysics scheme in WRF-Chem contributions to
671 AQMEII phase 2. *Atmospheric Environment*, In preparation.
- 672
673 Beltman, J.B., Hendriks, C., Tum, M., Schaap, M., 2013. The impact of large scale biomass
674 production on ozone air pollution in Europe. *Atmospheric Environment*, 71, 352-363.
- 675
676 Bianconi, R., Galmarini, S., Bellasio, R., 2004. Web-based system for decision support
677 in case of emergency: ensemble modelling of long-range atmospheric dispersion
678 of radionuclides. *Environmental Modelling and Software* 19, 401-411.
- 679
680 Binkowski, F.S., Arunachalam, S., Adelman, Z., Pinto, J., 2007. Examining photolysis rates
681 with a prototype on-line photolysis module in CMAQ. *Journal of Applied Meteorology and*
682 *Climatology*. 46, 1252-1256.
- 683
684 Brunner, D., Jorba, O., Savage, N., Eder, B., Makar, P., Giordano, L., Badia, A., Balzarini, A.,
685 Baro, R., Bianconi, R., Chemel, C., Forkel, R., Jimenez-Guerrero, P., Hirtl, M., Hodzic, A.,
686 Honzak, L., Im, U., Knote, C., Kuenen, J.J.P., Makar, P.A., Manders-Groot, A., Neal, L.,
687 Perez, J.L., Pirovano, G., San Jose, R., Savage, N., Schroder, W., Sokhi, R.S., Syrakov, D.,
688 Torian, A., Werhahn, K., Wolke, R., van Meijgaard, E., Yahya, K., Zabkar, R., Zhang, Y.,
689 Zhang, J., Hogrefe, C., Galmarini, S., 2014. Evaluation of the meteorological performance of
690 coupled chemistry-meteorology models in phase 2 of the Air Quality Model Evaluation
691 International Initiative. *Atmospheric Environment*, to be submitted.
- 692
693 Curci, G., Beekman, M., Vautard, R., Smiatek, G., Steinbrecher, R., Theloke, J., Friedrich, R.,
694 2009. Modelling study of the impact of isoprene and terpene biogenic emissions on European
695 ozone levels. *Atmospheric Environment*, 43, 1444-1455.
- 696
697 Dave, J.V., 1972. Development of programs for computing characteristics of ultraviolet
698 radiation, Final Report under Contract NAS5-21680, NASA Report CR-139134, National
699 Aeronautics and Space Administration, Goddard Space Flight Center, Greenbelt, Maryland,
700 NTIS # N75-10746/6SL, 27 pp.
- 701
702 European Environmental Agency, 2013. Air pollution by ozone across Europe during summer
703 2012. Overview of exceedances of EC ozone threshold values for April–September 2012.
704 EEA Technical report, No 3/2013, 52 pp.
- 705
706 Emmons, L. K., Walters, S., Hess, P. G., Lamarque, J.-F., Pfister, G. G., Fillmore, D.,
707 Granier, C., Guenther, A., Kinnison, D., Laepple, T., Orlando, J. J., Tie, X., Tyndall, G.,
708 Wiedinmyer, C., Baughcum, S. L., Kloster, S., 2010. Description and evaluation of the Model
709 for Ozone and Related chemical Tracers, version 4 (MOZART-4). *Geoscientific Model*

- 710 Development, 3, 43–67.
711
- 712 Flemming, J., Inness, A., Flentje, H., Huijnen, V., Moinat, P., Schultz, M. G., Stein, O., 2009.
713 Coupling global chemistry transport models to ECMWF’s integrated forecast system.
714 Geoscientific Model Development, 2, 253–265.
715
- 716 Forkel, R., Balzarini, A., Baró, R., Curci, G., Jiménez-Guerrero, P., Hirtl, M., Honzak, L.,
717 Im, U., Lorenz, C., Pérez, J.L., Pirovano, G., San José, R., Tuccella, P., Werhahn, J., Žabkar,
718 R., 2104. Analysis of the WRF-Chem contributions to AQMEII phase2 with respect to
719 aerosol radiative feedbacks on meteorology and pollutant distribution. Atmospheric
720 Environment, Submitted.
721
- 722 Galmarini, S., Bianconi, R., Addis, R., Andronopoulos, S., Astrup, P., Bartzis, J.C., Bellasio,
723 R., Buckley, R., Champion, H., Chino, M., D’Amours, R., Davakis, E., Eleveld, H., Glaab,
724 H., Manning, A., Mikkelsen, T., Pechinger, U., Polreich, E., Prodanova, M., Slaper, H.,
725 Syrakov, D., Terada, H., Van der Auwera, L., 2004a. Ensemble dispersion forecasting, Part II:
726 application and evaluation. Atmospheric Environment, 38 (28), 4619-4632.
727
- 728 Galmarini, S., Bianconi, R., Klug, W., Mikkelsen, T., Addis, R., Andronopoulos, S., Astrup,
729 P., Baklanov, A., Bartniki, J., Bartzis, J.C., Bellasio, R., Bompay, F., Buckley, R., Bouzom,
730 M., Champion, H., D’Amours, R., Davakis, E., Eleveld, H., Geertsema, G.T., Glaab, H.,
731 Kollax, M., Ilvonen, M., Manning, A., Pechinger, U., Persson, C., Polreich, E., Potemski, S.,
732 Prodanova, M., Saltbones, J., Slaper, H., Sofiev, M.A., Syrakov, D., Sørensen, J.H., Van der
733 Auwera, L., Valkama, I., Zelazny, R., 2004b. Ensemble dispersion forecasting, Part I:
734 concept, approach and Indicators. Atmospheric Environment, 38 (28), 4607-4617.
735
- 736 Galmarini, S., Rao, S.T., 2011. The AQMEII two-continent Regional Air Quality Model
737 evaluation study: Fueling ideas with unprecedented data. Atmospheric Environment, 45,
738 2464.
739
- 740 Galmarini, S., Bianconi, R., Appel, W., Solazzo, E., et al., 2012. ENSEMBLE and AMET:
741 two systems and approaches to a harmonised, simplified and efficient assistance
742 to air quality model developments and evaluation. Atmospheric Environment, 53, 51-59.
743
- 744 Giordano, L., Brunner, D., Flemming, J., Im, U., Hogrefe, C., Bianconi, R., Badia, A.,
745 Balzarini, A., Baro, R., Belassio, R., Chemel, C., Curci, G., Forkel, R., Jimenez-Guerrero, P.,
746 Hirtl, M., Hodzic, A., Honzak, L., Jorba, O., Knote, C., Kuenen, J.J.P., Makar, P.A., Manders-
747 Groot, A., Neal, L., Perez, J.L., Piravano, G., Pouliot, G., San Jose, R., Savage, N., Schroder,
748 W., Sokhi, R.S., Syrakov, D., Torian, A., Werhahn, K., Wolke, R., Yahya, K., Zabkar, R.,
749 Zhang, Y., Zhang, J., Galmarini, S., 2014. Assessment of the MACC/IFS-MOZART model
750 and its influence as boundary conditions on AQMEII phase 2 modelling domains.
751 Atmospheric Environment, Submitted.
752
- 753 Grell, G.A., Peckham, S.E., Schmitz, R., McKeen, S.A., Frost, G., Skamarock, W.C., Eder,
754 B., 2005. Fully coupled “online” chemistry within the WRF model. Atmospheric
755 Environment, 39, 6957-6975.
756
- 757 Guenther, A., Karl, T., Harley, P., Wiedinmyer, C., Palmer, P.I., Geron, C., 2006. Estimates
758 of global terrestrial isoprene emissions using MEGAN (Model of Emissions of Gases and
759 Aerosols from Nature. Atmospheric Chemistry and Physics, 6, 3181-3210.

- 760
761 Guenther, A.B., Zimmerman, P.R., Harley, P.C., Monson, R.K., Fall, R., 1993. Isoprene and
762 monoterpene rate variability: model evaluations and sensitivity analyses. *Journal of*
763 *Geophysical Research*, 98, D7, 12609-12617.
- 764
765 Hodzic, A., Madronich, S., Bohn, B., Massie, S., Menut, L., Wiedinmyer, C., 2007. Wildfire
766 particulate matter in Europe during summer 2003: meso-scale modeling of smoke emissions,
767 transport and radiative effects. *Atmospheric Chemistry and Physics*, 7 (15), 4043-4064.
- 768
769 Hogrefe, C., Roselle, S., Mathur, R., Rao, S.T., Galmarini, S., 2014. Space-time analysis of
770 the Air Quality Model Evaluation International Initiative (AQMEII) Phase 1 air quality
771 simulations. *Journal of Air Waste Management Association*, 64, 388-405.
- 772
773 Holtzlag, A. A. M. , Svensson, G., Baas, P. , Basu, S. , Beare, B. , Beljaars, A. C. M. ,
774 Bosveld, F. C. ,Cuxart, J., Lindvall, J. , Steeneveld, G. J. , Tjernström, M. , Van De Wiel, B.
775 J. H. , 2013. Stable Atmospheric Boundary Layers and Diurnal Cycles: Challenges for
776 Weather and Climate Models. *Bulletin of American Meteorological Society*, 94, 1691–1706.
- 777
778 Im, U., Bianconi, R., Solazzo, E., Kioutsioukis, I., Badia, A., Balzarini, A., Baro, R., Bellasio,
779 R., Brunner, D., Chemel, C., Curci, G., Denier van der Gon, H.A.C., Flemming, J., Forkel, R.,
780 Giordano, L., Jimenez-Guerrero, P., Hirtl, M., Hodzic, A., Honzak, L., Jorba, O., Knote, C.,
781 Makar, P.A., Manders-Groot, A., Neal, L., Perez, J.L., Pirovano, G., Pouliot, G., San Jose, R.,
782 Savage, N., Schroder, W., Sokhi, R.S., Syrakov, D., Torian, A., Tuccella, P., Werhahn, K.,
783 Wolke, R., Yahya, K., Zabkar, R., Zhang, Y., Zhang, J., Hogrefe, C., Galmarini, S., 2014.
784 Evaluation of operational online-coupled regional air quality models over Europe and North
785 America in the context of AQMEII phase 2. Part II: Particulate Matter. *Atmospheric*
786 *Environment*, <http://dx.doi.org/10.1016/j.atmosenv.2014.08.072>, In Press.
- 787
788 Inness, A., Baier, F., Benedetti, A., Bouarar, I., Chabrillat, S., Clark, H., Clerbaux, C.,
789 Coheur, P., Engelen, R. J., Errera, Q., Flemming, J., George, M., Granier, C., Hadji-Lazaro,
790 J., Huijnen, V., Hurtmans, D., Jones, L., Kaiser, J. W., Kapsomenakis, J., Lefever, K., Leitão,
791 J., Razinger, M., Richter, A., Schultz, M. G., Simmons, A. J., Suttie, M., Stein, O., Thépaut,
792 J.-N., Thouret, V., Vrekoussis, M., Zerefos, C., and the MACC team, 2013. The MACC
793 reanalysis: an 8 yr data set of atmospheric composition. *Atmospheric Chemistry and Physics*,
794 13, 4073-4109.
- 795
796 Jorba, O., Dabdub, D., Blaszczyk-Boxe, C., Pérez, C., Janjic, Z., Baldasano, J. M., Spada, M.,
797 Badia, A., Gonçalves, M., 2012. Potential Significance of Photoexcited NO₂ on Global Air
798 Quality with the NMMB/BSC Chemical Transport Model. *Journal of Geophysical Research*,
799 117.
- 800
801 Karl, M., Dorn, H.-P., Holland, F., Koppmann, R., Poppe, D., Rupp, L., Schaub, A. &
802 Wahner, A., 2006. Product study of the reaction of OH radicals with isoprene in the
803 atmosphere simulation chamber SAPHIR. *Journal of Atmospheric Chemistry* 55 (2), 167-187.
- 804
805 Kim, Y., Sartelet K., Seigneur C., 2009. Comparison of two gas-phase chemical kinetic
806 mechanisms of ozone formation over Europe. *Journal of Atmospheric Chemistry*, 62, 89–119.

- 807 Kim, Y., Sartelet, K., Seigneur, C., 2011. Formation of secondary aerosols over Europe:
808 comparison of two gas-phase chemical mechanisms. *Atmospheric Chemistry and Physics*, 11,
809 583–598.
- 810 Kioutsioukis, I., Im, U., Bianconi, R., Badia, A., Balzarini, A., Baró, R., Bellasio, R.,
811 Brunner, D., Chemel, C., Curci, G., Denier van der Gon, H., Flemming, J., Forkel, R.,
812 Giordano, L., Jiménez-Guerrero, P., Hirtl, M., Jorba, O., Manders-Groot, A., Neal, L., Pérez,
813 J.L., Piravano, G., San Jose, R., Savage, N., Schroder, W., Sokhi, R.S., Solazzo, E., Syrakov,
814 D., Tuccella, P., Werhahn, J., Wolke, R., Hogrefe, C., Galmarini, S., 2014. Challenges in the
815 deterministic skill of air quality ensembles. *Atmospheric Environment*, Submitted.
- 816
- 817 Kioutsioukis, I., Galmarini, S., 2014. De praeceptis ferendis: good practice in multi-model
818 ensembles. *Atmospheric Chemistry and Physics Discussions*, Submitted.
- 819
- 820 Knote, C., Hodzic, A., Jimenez, J. L., Volkamer, R., Orlando, J. J., Baidar, S., Brioude, J.,
821 Fast, J., Gentner, D. R., Goldstein, A. H., Hayes, P. L., Knighton, W. B., Oetjen, H., Setyan,
822 A., Stark, H., Thalman, R., Tyndall, G., Washenfelder, R., Waxman, E., Zhang, Q., 2013.
823 Simulation of semi-explicit mechanisms of SOA formation from glyoxal in a 3-D model.
824 *Atmospheric Chemistry and Physics Discussions*, 13, 26699-26759.
- 825
- 826 Kuenen, J.J.P., Visschedijk, A.J.H., Jozwicka, M., Denier van der Gon, H.A.C., 2014.
827 TNO_MACC_II emission inventory: a multi-year (2003-2009) consistent high-resolution
828 European emission inventory for air quality modelling. *Atmospheric Chemistry and Physics*
829 *Discussions*, 14, 5837-5869.
- 830
- 831 Lurmann, F. W., I. Loyd, A. C. Atkinson, R., 1986. A chemical mechanism for use in
832 long-range transport/acid deposition computer modeling. *Journal of Geophysical*
833 *Research* 91, 10 905-10 936.
- 834
- 835 Makar, P.A., Gong, W., Hogrefe, C., Zhang, Y., Curci, G., Zabkar, R., Milbrandt, J., Im, U.,
836 Galmarini, S., Balzarini A., Baro, R., Bianconi, R., Cheung, P., Forkel, R., Gravel, S., Hirtl,
837 M., Honzak, L., Hou, A., Jimenez-Guerrero, P., Langer M., Moran, M.D., Pabla, B., Perez,
838 P.L., Pirovano, G., San Jose, R., Tuccella, P., Werhahn, J., Zhang, J., 2014a. Feedbacks
839 between Air Pollution and Weather, Part 1: Effects on Chemistry. *Atmospheric Environment*,
840 Submitted.
- 841
- 842 Makar, P.A., Gong, W., Hogrefe, C., Zhang, Y., Curci, G., Zabkar, R., Milbrandt, J., Im, U.,
843 Galmarini, S., Balzarini A., Baro, R., Bianconi, R., Cheung, P., Forkel, R., Gravel, S., Hirtl,
844 M., Honzak, L., Hou, A., Jimenez-Guerrero, P., Langer M., Moran, M.D., Pabla, B., Perez,
845 P.L., Pirovano, G., San Jose, R., Tuccella, P., Werhahn, J., Zhang, J., 2014b. Feedbacks
846 between Air Pollution and Weather, Part 2: Effects on Weather. *Atmospheric Environment*,
847 Submitted.
- 848
- 849 Makar, P.A., Moran, M.D., Zheng, Q., Cousineau, S., Sassi, M., Duhamel, A., Besner, M.,
850 Davignon, D., Crevier, L.-P., Bouchet, V.S., 2009. Modelling the impacts of ammonia
851 emissions reductions on North American air quality. *Atmospheric Chemistry and Physics*, 9
852 (18), 7183-7212.
- 853
- 854 O'Connor, F. M., Johnson, C. E., Morgenstern, O., Abraham, N. L., Braesicke, P., Dalvi, M.,
855 Folberth, G. A., Sanderson, M. G., Telford, P. J., Voulgarakis, A., Young, P. J., Zeng, G.,

- 856 Collins, W. J., Pyle, J. A., 2014. Evaluation of the new UKCA climate-composition model –
857 Part 2: The Troposphere. *Geoscientific Model Development*, 7, 41-91.
858
- 859 Poppe, D., Andersson-Sköld, Y., Baart, A., Builtjes, P.J.H., Das, M., Fiedler, F., Hov, O.,
860 Kirchner, F., Kuhn, M., Makar, P.A., Milford, J.B., Roemer, M.G.M., Ruhnke, R., Simpson,
861 D., Stockwell, W.R., Strand, A., Vogel, B., Vogel, H., 1996. Gas-phase reactions in
862 atmospheric chemistry and transport models: a model intercomparison. Eurotrac report. ISS,
863 Garmisch-Partenkirchen.
864
- 865 Pouliot, G., Pierce, T., Denier van der Gon, H., Schaap, M., Moran, M., Nopmongcol, U.,
866 2012. Comparing emissions inventories and model-ready emissions datasets between Europe
867 and North America for the AQMEII Project. *Atmospheric Environment* 53, 75-92.
868
- 869 Pouliot, G., Denier van der Gon, H., Kuenen, J., Makar, P., Zhang, J., Moran, M., 2014.
870 Analysis of the Emission Inventories and Model-Ready Emission Datasets of Europe and
871 North America for Phase 2 of the AQMEII Project. *Atmospheric Environment*, Submitted.
872
- 873 Qian, Y., Gustafson, Jr. W.I., Fast, J.D., 2010. An investigation of the sub-grid variability of
874 trace gases and aerosols for global climate modeling. *Atmospheric Chemistry and Physics*, 10,
875 6917-6946.
876
- 877 Reidmiller, D.R., Fiore, A.M., Jaffe, D.A., Bergmann, D., Cuvelier, C., Dentener, F.J.,
878 Duncan, B.N., Folberth, G., Gauss, M., Gong, S., Hess, P., Jonson, J.E., Keating, T., Lupu,
879 A., Marmer, E., Park, R., Schultz, M.G., Shindell, D.T., Szopa, S., Vivanco, M.G., Wild, O.,
880 Zuber, A., 2009. The influence of foreign vs. North American emissions on surface ozone in
881 the US. *Atmospheric Chemistry and Physics*, 9, 5027-5042.
882
- 883 Russell, A., Dennis, R., 2000. NARSTO critical review of photochemical models and
884 modelling. *Atmospheric Environment* 34, 2283-2324.
885
- 886 Sarwar, G., Appel, K. W., Carlton, A. G., Mathur, R., Schere, K., Zhang, R., Majeed, M. A.,
887 2011. Impact of a new condensed toluene mechanism on air quality model predictions in the
888 US. *Geoscientific Model Development*, 4, 183-193.
889
- 890 Sassi, M., Chen, J., Samaali, M., Davignon, D., Moran, M.D., Taylor, B., Zheng, Q., 2010.
891 2006 Canadian emissions for air quality modelling, 19th International Emission Inventory
892 Conference, 27-30 September, 2010, San Antonio, Texas, US.
893
- 894 Sauter, F., van der Swaluw, E., Manders-Groot, A., Wichink Kruit, R., Segers, A., Eskes, H.,
895 2012. LOTOS-EUROS v1.8 Reference Guide. TNO report TNO-060-UT-2012-01451, TNO.
896
- 897 Savage, N. H., Agnew, P., Davis, L. S., Ordóñez, C., Thorpe, R., Johnson, C. E., O'Connor, F.
898 M., Dalvi, M., 2013. Air quality modelling using the Met Office Unified Model (AQU
899 OS24-26): model description and initial evaluation. *Geoscientific Model Development*, 6,
900 353-372.
901
- 902 Schaap, M., M. Roemer, F. Sauter, G. Boersen, R. Timmermans, P.J.H. Builtjes, LOTOS-
903 EUROS: Documentation, TNO report B&O-A, 2005-297, Apeldoorn 2005
904

- 905 Schwede, D., Pouliot, G., Pierce, T., 2005. Changes to the Biogenic Emissions Inventory
906 System version 3 (BEIS3). In: 4th CMAS Models-3 Users' Conference, Chapel Hill, NC, 26–
907 28 September 2005.
- 908
909 Schere, K., Flemming, J., Vautard, R., Chemel, C., Colette, A., Hogrefe, C., Bessagnet, B.,
910 Meleux, F., Mathur, R., Roselle, S., Hu, R.-M., Sokhi, R. S., Rao, S.T., S. Galmarini, 2012:
911 Trace gas/aerosol boundary concentrations and their impacts on continental-scale AQMEII
912 modeling domains, *Atmospheric Environment*, 53, 38-50.
- 913
914 Sillman, S., Samson, P.J., 1995. Impact of temperature on oxidant photochemistry in urban,
915 polluted rural and remote environments. *Journal of Geophysical Research: Atmospheres*, 100,
916 D6, 11497–11508.
- 917
918 Soares, J., Sofiev, M., Prank, M., San Jose, R., Perez, J.L., 2014. On uncertainties of wild-land
919 fires emission in AQMEII case study. *Atmospheric Environment*, In preparation.
- 920
921 Sofiev, M., Vankevich, R., Lotjonen, M., Prank, M., Petukhov, V., Ermakova, T., Koskinen,
922 J., Kukkonen, J., 2009. An operational system for the assimilation of the satellite information
923 on wild-land fires for the needs of air quality modelling and forecasting. *Atmospheric
924 Chemistry and Physics*, 9, 6833-6847.
- 925
926 Solazzo, E., Riccio, A., Kioutsioukis, I., Galmarini, S., 2013b. Pauci ex tanto numero: reduce
927 redundancy in multi-model ensembles. *Atmospheric Chemistry and Physics*, 13, 8315-8333.
- 928
929 Solazzo, E., Bianconi, R., Pirovano, G., Moran, M. D., Vautard, R., Hogrefe, C., Appel, K.
930 W., Matthias, V., Grossi, P., Bessagnet, B., Brandt, J., Chemel, C., Christensen, J. H., Forkel,
931 R., Francis, X. V., Hansen, A. B., McKeen, S., Nopmongcol, U., Prank, M., Sartelet, K. N.,
932 Segers, A., Silver, J. D., Yarwood, G., Werhahn, J., Zhang, J., Rao, S. T., Galmarini, S.,
933 2013a. Evaluating the capability of regional-scale air quality models to capture the vertical
934 distribution of pollutants. *Geoscientific Model Development*, 6, 791-818.
- 935
936 Solazzo, E., Bianconi, R., Vautard, R., Appel, K. W., Moran, M. D., Hogrefe, C., Bessagnet,
937 B., Brandt, J., Christensen, J. H., Chemel, C., Coll, I., van der Gon, H. D., Ferreira, J.,
938 Forkel, R., Francis, X. V., Grell, G., Grossi, P., Hansen, A. B., Jericevic, A., Kraljevic, L.,
939 Miranda, A. I., Nopmongcol, U., Pirovano, G., Prank, M., Riccio, A., Sartelet, K. N., Schaap,
940 M., Silver, J. D., Sokhi, R. S., Vira, J., Werhahn, J., Wolke, R., Yarwood, G., Zhang, J., Rao,
941 S.T., Galmarini, S., 2012. Ensemble modelling of surface level ozone in Europe and North
942 America in the context of AQMEI. *Atmospheric Environment*, 53, 60–74.
- 943
944 Stockwell, W. R., Kirchner, F., Kuhn, M., Seefeld, S., 1997. A new mechanism for regional
945 atmospheric chemistry modeling. *Journal of Geophysical Research*, 102, 25847-25879.
- 946
947 Stockwell, W. R., P. Middleton, J. S. Chang, and X. Tang, 1990. The second generation
948 regional acid deposition model chemical mechanism for regional air quality modeling.
949 *Journal of Geophysical Research*, 95, 16343-16367.
- 950
951 Tie, X., Madronich, S., Walters, S., Zhang, R., Rasch, P., Collins, W., 2003. Effects of clouds
952 on photolysis and oxidants in the troposphere. *Journal of Geophysical Research*, 108, D20,
953 4642.
- 954

- 955 Vautard, R., Moran, M. D., Solazzo, E., Gilliam, R. C., Matthias, V., Bianconi, R., Chemel,
956 C., Ferreira, J., Geyer, B., Hansen, A. B., Jericevic, A., Prank, M., Segers, A., Silver, J. D.,
957 Werhahn, J., Wolke, R., Rao, S. T., Galmarini, S., 2012. Evaluation of the meteorological
958 forcing used for AQMEII air quality simulations, *Atmospheric Environment*, 53, 15–37.
959
- 960 Visschedijk, A.J.H., Zandveld, P., Denier van der Gon, H.A.C., 2007. A High Resolution
961 Gridded European Emission Database for the EU Integrated Project GEMS. TNO
962 report 2007-A-R0233/B.
963
- 964 Vogel, B., Vogel, H., Baumer, D., Bangert, M., Lundgren, K., Rinke, R., Stanelle, T., 2009.
965 The comprehensive model system COSMO-ART – Radiative impact of aerosol on the state of
966 the atmosphere on the regional scale. *Atmospheric Chemistry and Physics*, 9, 8661–
967 8680.
968
- 969 Wang, K., Yahya, K., Zhang, Y., Wu, S.-Y., Grell, G., 2014. Implementation and Initial
970 Application of A New Chemistry-Aerosol Option in WRF/Chem for Simulation of Secondary
971 Organic Aerosols and Aerosol Indirect Effects. *Atmospheric Environment*, Under review.
972
- 973 Whitten, G. Z., Heo, G., Kimura, Y., McDonald-Buller, E., Allen, D., Carter, W. P. L.,
974 Yarwood, G., 2010. A new condensed toluene mechanism for Carbon Bond: CB05-TU.
975 *Atmospheric Environment*, 44, 5346–5355, 2010.
976
- 977 Wiedinmyer, C., Akagi, S. K., Yokelson, R. J., Emmons, L. K., Al-Saadi, J. A., Orlando, J. J.,
978 Soja, A. J., 2011. The Fire INventory from NCAR (FINN): a high resolution global model to
979 estimate the emissions from open burning, *Geoscientific Model Development*, 4, 625-641.
980
- 981 Wild, O., Zhu, X., Prather, M.J., 2000. FAST-J: accurate simulation of in- and below-cloud
982 photolysis in tropospheric chemical models. *Journal of Atmospheric Chemistry* 37, 245–282.
983
- 984 Wolf, M.E., Fields, P.G., Manne, G.K., Villegas, M.T.L., Bravo, V.G., Gomez, R.I., 2009.
985 Developing Mexico National Emissions Inventory Projections for the Future Years of 2008,
986 2012, and 2030, 18th International Emission Inventory Conference, 14-17 August, 2009,
987 Baltimore, Maryland.
988
- 989 Wolke, R., Schroder, W., Schrodner, R., Renner, E., 2012. Influence of grid resolution and
990 meteorological forcing on simulated European air quality: a sensitivity study with the
991 modeling system COSMO–MUSCAT. *Atmospheric Environment* 53, 110–130.
992
- 993 Wong, D. C., Pleim, J., Mathur, R., Binkowski, F., Otte, T., Gilliam, R., Pouliot, G., Xiu, A.,
994 Young, J. O., Kang, D., 2012. WRF-CMAQ two-way coupled system with aerosol feedback:
995 software development and preliminary results. *Geoscientific Model Development*, 5, 299-312.
996
- 997 Yahya, K., Wang, K., Gudoshava, M., Glotfelty, T., Zhang, Y., 2014a. Application of
998 WRF/Chem over the continental U.S. under the AQMEII Phase II: Comprehensive Evaluation
999 of 2006 Simulation. *Atmospheric Environment*,
1000 <http://dx.doi.org/10.1016/j.atmosenv.2014.08.063>, In Press.
1001
- 1002 Yahya, K., Wang, K., Zhang, Y., Kleindienst, T. E., 2014b. Application of WRF/Chem over
1003 the continental U.S. under the AQMEII Phase II: Comprehensive Evaluation of 2010

- 1004 Simulation and Responses of Air Quality and Meteorology-Chemistry Interactions to Changes
1005 in Emissions and Meteorology from 2006 to 2010. Atmospheric Environment, Under review.
1006
- 1007 Yarwood, G., Rao, S., Yocke, M., Whitten, G. Z., 2005. Updates to the Carbon Bond
1008 chemical mechanism: CB05. Final Report to the US EPA, RT-0400675, 8 December 2005.
1009
- 1010 Zaveri, R.A., Peters, L.K., 1999. A new lumped structure photochemical mechanism for
1011 large-scale applications. Journal of Geophysical Research, 104, D23, 30387-30415.
1012
- 1013 Zhang, J., Zheng, Q., Moran, M.D., Gordon, M., Liggio, J., Makar, P.A., Taylor, B., Stroud,
1014 C., 2012. Improvements to SMOKE processing of Canadian On-Road mobile emissions, 20th
1015 International Emission Inventory Conference, 13-16 Aug. 2012, Tampa, Florida.
1016
- 1017 Zhang, Y., Sartelet, K., Zhu, S., Wang, W., Wu, S.-Y., Zhang, X., Wang, K., Tran, P.,
1018 Seigneur, C., Wang, Z.-F., 2013. Application of WRF/Chem-MADRID and
1019 WRF/Polyphemus in Europe – Part 2: Evaluation of chemical concentrations and sensitivity
1020 simulations. Atmospheric Chemistry and Physics, 13, 6845-6875.
1021
- 1022 Zhang, Y., 2008. Online Coupled Meteorology and Chemistry models: History, Current
1023 Status, and Outlook. Atmospheric Chemistry and Physics, 8, 2895-2932.
1024

Table 1. Modelling systems participated to AQMEII2 and their configurations

	Groups	Domain	Model	Grid Spacing	First layer height (m)	Biogenic Model	Gas Phase	Photolysis	Model Reference
M1	AT1	EU	WRF-CHEM	23 km	24	MEGAN	RADM2 ¹	Fast-J ¹³	Grell et al., 2005
M2	CH1	EU	COSMO-ART	0.22°	20	Gunther et al., 1998	RADM2K ²	GRAALS+STAR ²	Vogel et al., 2009
M3	DE3	EU	COSMO-MUSCAT	0.25°	20	Gunther et al., 1993	RACM-MIM2 ³	Fast-J	Wolke et al., 2012
M4	DE4	EU	WRF-CHEM	23 km	24	MEGAN	RADM2 modified ⁴	Fast-J	Grell et al., 2005; Forkel et al., 2014
M5	ES1	EU	WRF-CHEM	23 km	24	MEGAN	RADM2	Fast-J	Grell et al., 2005
M6	ES2a	EU	NMMB-BSC-CTM	0.20 °	45	MEGAN	CB05 ⁵	Fast-J	Jorba et al., 2012
M7	ES3	EU	WRF-CHEM	23 km	24	MEGAN	CBMZ ⁶	Fast-J	Grell et al., 2005
M8	IT1	EU	WRF-CHEM	23 km	24	MEGAN	CBMZ	Fast-J	Grell et al., 2005
M9	IT2	EU	WRF-CHEM	23 km	24	MEGAN	RACM ⁷	Fast-J	Grell et al., 2005
M10	NL2	EU	RACMO LOTOS-EUROS	0.5 ° × 0.25°	25	Beltman et al., 2013	CB-IV modified ⁸	Poppe et al., 1996	Sauter et al., 2012
M11	SI1	EU	WRF-CHEM	23 km	25	MEGAN	RADM2	Fast-J	Grell et al., 2005
M12	UK4	EU	MetUM-UKCA RAQ	0.22 °	20	TNO	UKCA RAQ ⁹	Fast-J	Savage et al., 2013
M13	CA2f	NA	GEM-MACH	15 km	20.66	BEIS	ADOM-II ¹⁰	Dave, 1972	Makar et al., 2014a,b
M14	US6	NA	WRF-CMAQ	12 km	19	BEIS3.14	CB05-TU ¹¹	Binkowski et al., 2007	Wong et al., 2012
M15	US7	NA	WRF-CHEM	36 km	55-60	MEGAN	MOZART ¹²	fTUV ¹⁴	Grell et al., 2005
M16	US8	NA	WRF-CHEM	36 km	38	MEGAN	CB05	fTUV	Grell et al., 2005; Wang et al., 2014

1 Stockwell et al. (1990); 2 Vogel et al. (2009); 3 Karl et al. (2006); 4 Forkel et al. (2014); 5 Yarwood et al. (2005); 6 Zaveri et al. (1999); 7 Stockwell et al. (1997); 8 Sauter et al. (2012); 9 Savage et al. (2013); 10 Lurmann et al. (1986); 11 Whitten et al., 2010; Sarwar et al., 2011; 12 Emmons et al. (2010); Knote et al. (2013); 13 Wild et al., 2000; 14 Tie et al., 2003

Table 2. Annual anthropogenic emissions (ktons km⁻² yr⁻¹) provided by TNO-MACC-II inventory and biogenic isoprene emissions (ktons km⁻² yr⁻¹) integrated over the EU and NA domains.

Species	EU	NA
CO	614	478
NO _x *	277	120
NMVOC	230	85
NH ₃	109	31
SO ₂	109	70
PM _{2.5}	49	29
PM ₁₀	69	76
ISOP**	2.4-24.9	0.02-8.1

* Only anthropogenic NO_x is reported.

**The groups that provided isoprene emissions are AT1, CH1, DE3, IT2, NL2 and UK4 for the EU domain and CA2f, US6 and US7 for the NA domain.

Table 3. Statistical comparisons of observed and simulated annual domain-mean hourly surface O₃ and domain- and annually-integrated O₃ dry deposition over EU and NA in 2010.

Members	<i>r</i>	<i>NMSE (%)</i>	<i>NMB (%)</i>	<i>RMSE*</i>	<i>Dry Deposition (Tg km⁻²)</i>
M1/AT1	0.86	2.66	-4.92	9.57	<i>NP</i>
M2/CH1	0.82	8.03	-18.30	15.42	0.28
M3/DE3	0.68	6.37	-2.12	15.02	0.13
M4/DE4	0.83	3.17	-1.64	10.62	2.24
M5/ES1	0.86	4.08	-11.41	11.44	2.18
M6/ES2a	0.83	6.37	-7.71	14.59	2.79
M7/ES3	0.86	4.29	-12.07	11.69	1.82
M8/IT1	0.85	4.57	-12.45	12.03	<i>NP</i>
M9/IT2	0.84	6.21	-15.80	13.76	1.77
M10/NL2	0.89	2.83	-4.34	9.90	0.14
M11/SI1	0.87	2.38	-3.78	9.10	1.91
M12/UK4	0.85	7.88	2.30	17.08	<i>NP</i>
EU Mean	0.86	3.22	-7.70	10.37	
EU Median	0.86	3.23	-8.69	10.33	
M13/CA2f	0.85	1.45	2.43	4.02	0.09
M14/US6	0.84	2.15	1.14	4.85	0.10
M15/US7	0.78	4.36	-4.56	6.72	0.15
M16/US8	0.88	8.11	-22.36	8.26	3.05
NA Mean	0.83	3.70	-11.98	5.94	
NA Median	0.87	2.62	-9.51	5.07	

* *RMSE* is in units of $\mu\text{g m}^{-3}$ for EU and ppb for NA.

Table 4. *NMB* calculated for vertical O₃ profiles for each model group and ensemble mean and median for the WOUDC stations in EU.

Stations	Station Name	Country	Lat/Lon	AT1	CH1	DE3	DE4	ES1	ES2a	ES3	IT1	IT2	NL2	SI1	UK4	Mean	Median
STN043	Lerwick	United Kingdom	60.1/-1.2	-8.40	-12.14	-27.80	-2.39	-9.82	-11.46	-7.86	-6.91	-9.05	-3.32	-8.16	-11.13	-10.40	-7.40
STN053	UCCLE	Belgium	50.8/4.4	-4.11	-10.09	-14.08	3.80	-6.02	-7.46	-4.14	-4.53	-7.23	-1.96	-3.95	-4.86	-5.50	-3.56
STN099	Hohenpeissenberg	Germany	47.8/11.0	-10.65	-21.94	-23.98	-2.04	-12.15	-11.98	-8.96	-9.55	-11.47	0.17	-10.39	-8.43	-11.62	-9.63
STN156	Payerne	Switzerland	46.5/6.6	1.18	-10.06	-11.71	11.77	-0.63	1.84	2.51	2.43	0.51	2.70	1.44	3.94	0.64	2.52
STN242	Praha	Czech Rep.	50.0/14.5	-8.55	-16.18	-26.48	-1.72	-11.38	-8.82	-6.98	-6.97	-8.68	-4.77	-7.86	-5.06	-9.50	-7.35
STN308	Barajas	Spain	40.5/-3.7	-6.02	-14.29	-9.83	1.91	-7.72	-4.77	-6.72	-6.32	-7.83	0.21	-5.67	-1.61	-5.95	-5.01
STN316	De Bilt	Netherlands	52.1/5.2	-4.57	-5.83	-9.82	3.62	-6.14	-4.29	-4.99	-5.08	-7.29	1.15	-4.37	-0.59	-4.23	-3.76
STN318	Valentia	Ireland	51.9/-10.3	-6.51	-10.56	-15.49	-0.44	-8.01	-9.30	-6.00	-2.93	-6.35	-5.74	-6.43	-5.97	-7.01	-5.04
STN348	Ankara	Turkey	40.0/32.9	-11.48	-16.13	-12.94	5.76	-13.38	-4.28	-10.95	-11.12	-15.24	0.55	-11.36	2.41	-8.66	-9.74

Table 5. *NMB* calculated for vertical O₃ profiles for each model group and ensemble mean and median for the WOUDC stations in NA.

Stations	Station Name	Country	Lat/Lon	CA2f	US6	US7	US8	Mean	Median
STN021	Stony Plain	Canada	53.4/-114.1	-9.82	1.58	-2.29	-4.71	-3.81	-2.85
STN107	Wallops Island	USA	37.9/-75.5	-10.19	1.77	-1.17	-13.52	-5.78	-6.30
STN338	Bratts Lake	Canada	50.2/-104.8	-14.29	0.27	-3.26	-9.46	-6.68	-4.47
STN456	Egbert	Canada	44.2/-79.8	-16.78	-1.40	-3.95	-15.01	-9.28	-8.54
STN457	Kelowna	Canada	49.9/-119.4	-10.09	13.61	4.95	-0.62	1.96	2.05
STN458	Yarmouth	Canada	43.9/-66.1	-17.76	-1.17	-5.95	-15.27	-10.04	-10.20

Figure Captions

Fig.1. Annual NO_x emissions (tonnes/grid) overlaid with the rural monitoring stations used for model performance evaluation in EU (a) and in NA (b). The red circles show EU1/NA1, yellow diamonds show EU2/NA2, green squares show EU3/NA3 and black triangles show EU4/NA4.

Fig.2. Observed and simulated annual mean diurnal profiles (a,d), box plots (b,e) and soccer diagrams (c,f) for surface levels ozone mixing ratios in EU (upper panel) and NA (lower panel). Mn and Md represent the mean and median ensembles, respectively. EU0 and NA0 represent the two respective continents. Different colors represent the different sub-regions. Note the differences in scales.

Fig.3. Geographical distributions of observed and simulated annual surface level ozone mixing ratios in EU. Note the differences in scales.

Fig.4. Geographical distributions of observed and simulated annual surface level ozone mixing ratios in NA. Note the differences in scales.

Fig.5. Soccer diagrams for the seasonal and geographical model performances in EU: a) winter, b) spring, c) summer and d) autumn. Mn and Md represent the mean and median ensembles, respectively. EU0 and NA0 represent the continental levels. Different colors represent the different sub-regions. Note the differences in scales.

Fig.6. Soccer diagrams for the seasonal and geographical model performances in NA: a) winter, b) spring, c) summer and d) autumn. Mn and Md represent the mean and median ensembles, respectively. EU0 and NA0 represent the continental levels. Different colors represent the different sub-regions. Note the differences in scales.

Fig.7. Observed and simulated seasonal diurnal O_3 profiles in a) winter, b) spring, c) summer and d) autumn over EU2.

Fig.8. Observed and simulated seasonal diurnal O_3 profiles in a) winter, b) spring, c) summer and d) autumn over NA3.

Fig.9. Observed surface O_3 concentration bins against mean bias for the EU and NA domains for the O_3 season (May-September).

Fig.10. Observed and simulated (models, mean and median) vertical O_3 profiles averaged over 2010 in the EU domain. Note the differences in scales.

Fig.11. Observed and simulated (models, mean and median) vertical O_3 profiles averaged over 2010 in the NA domain. Note the differences in scales.

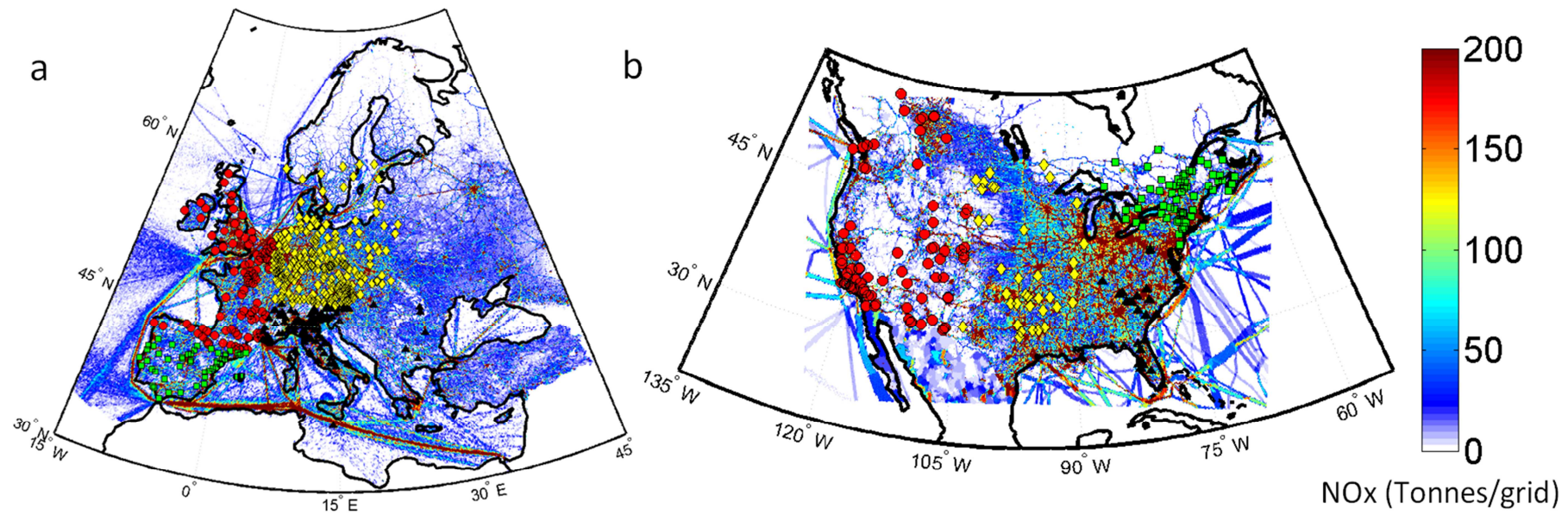


Fig.1.

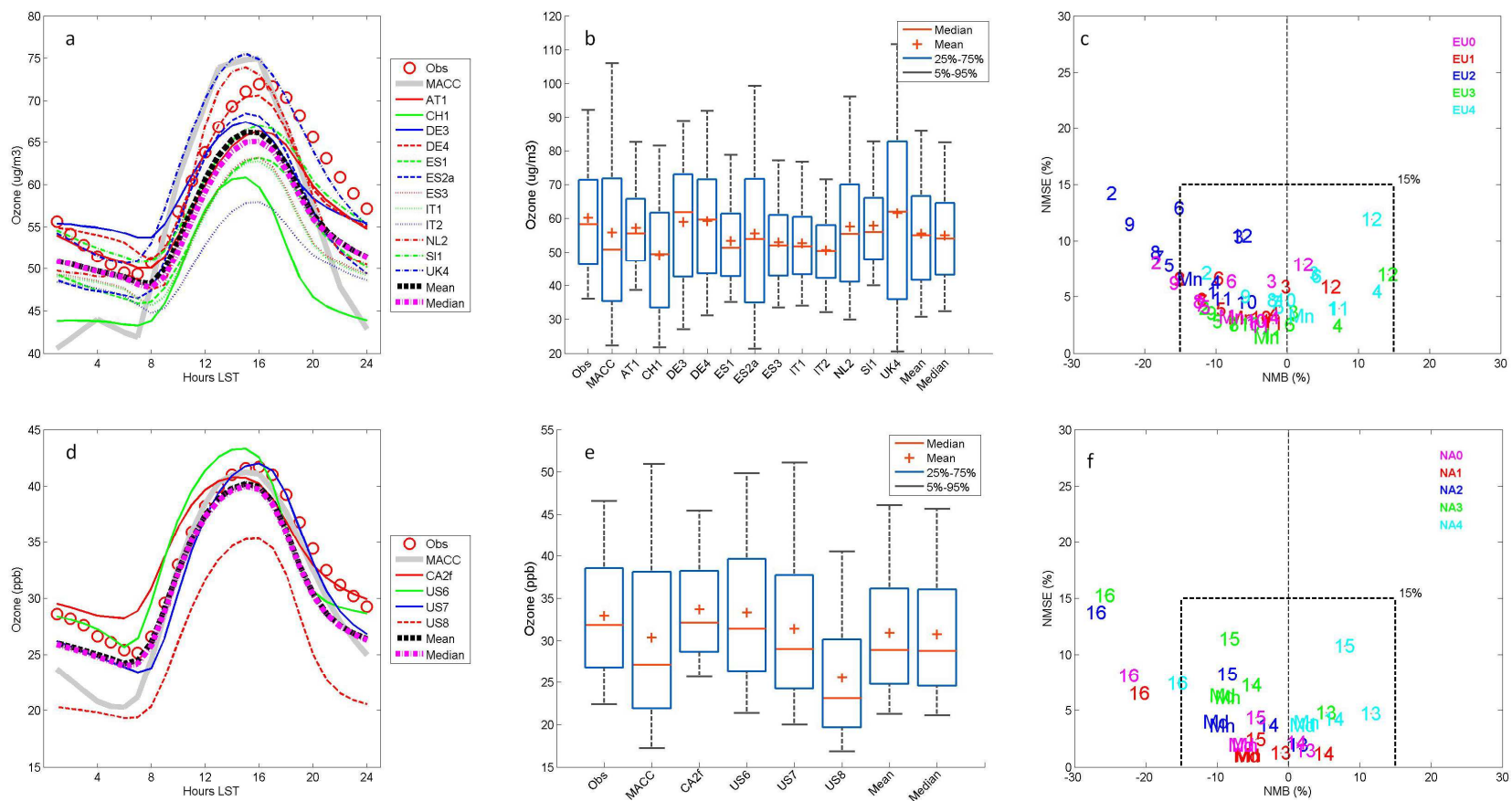


Fig.2.

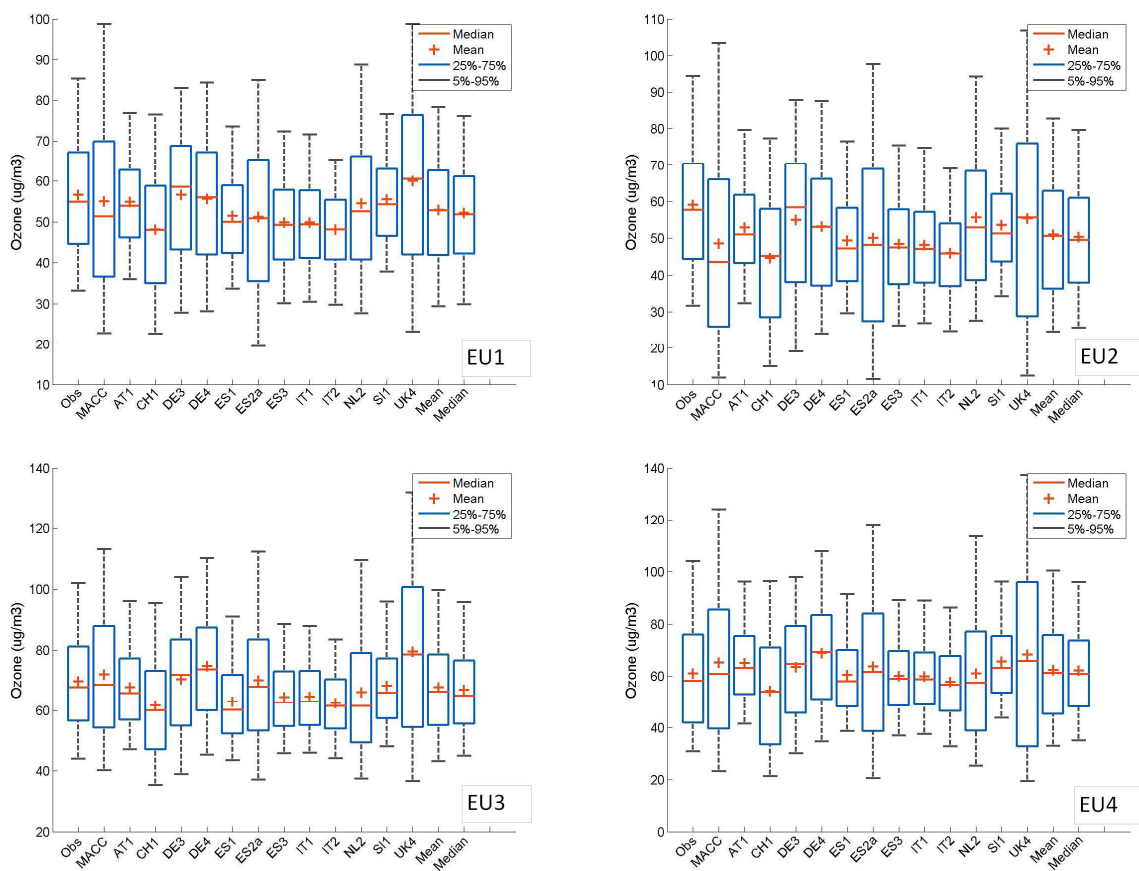


Fig.3.

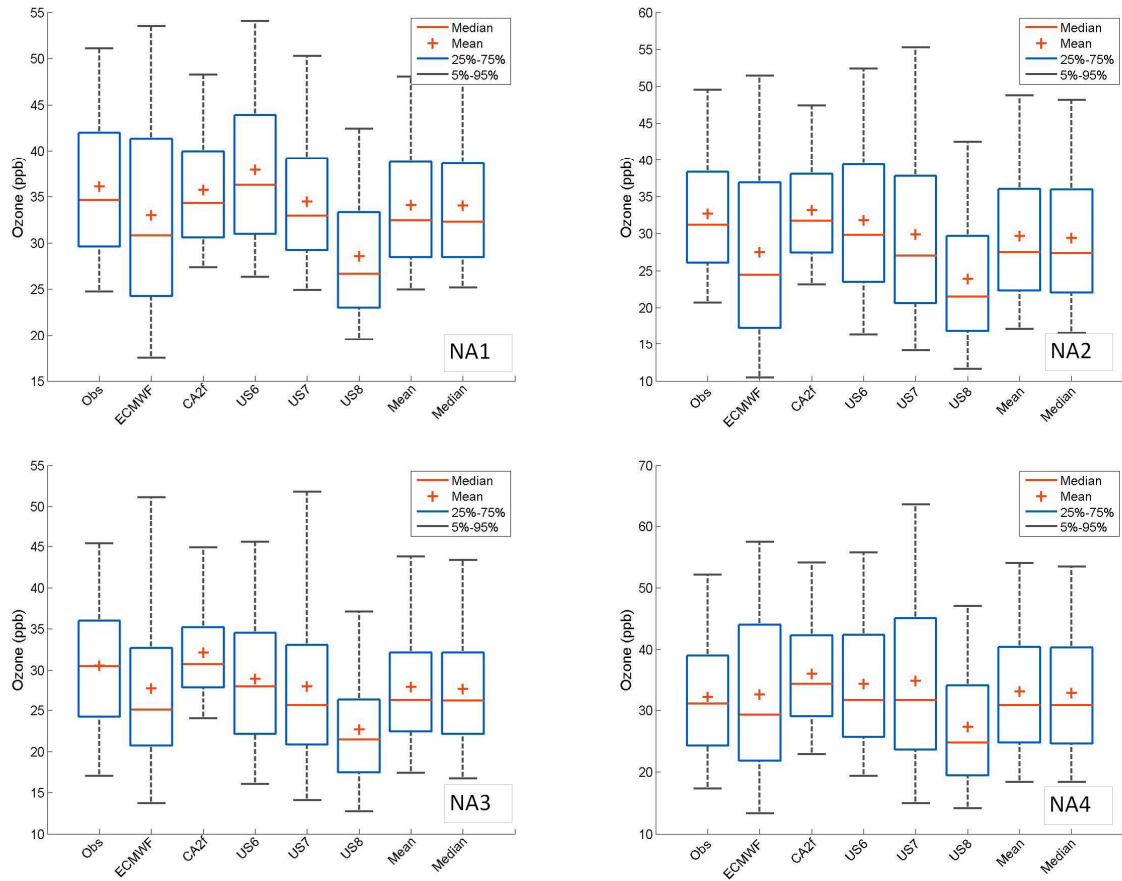


Fig.4.

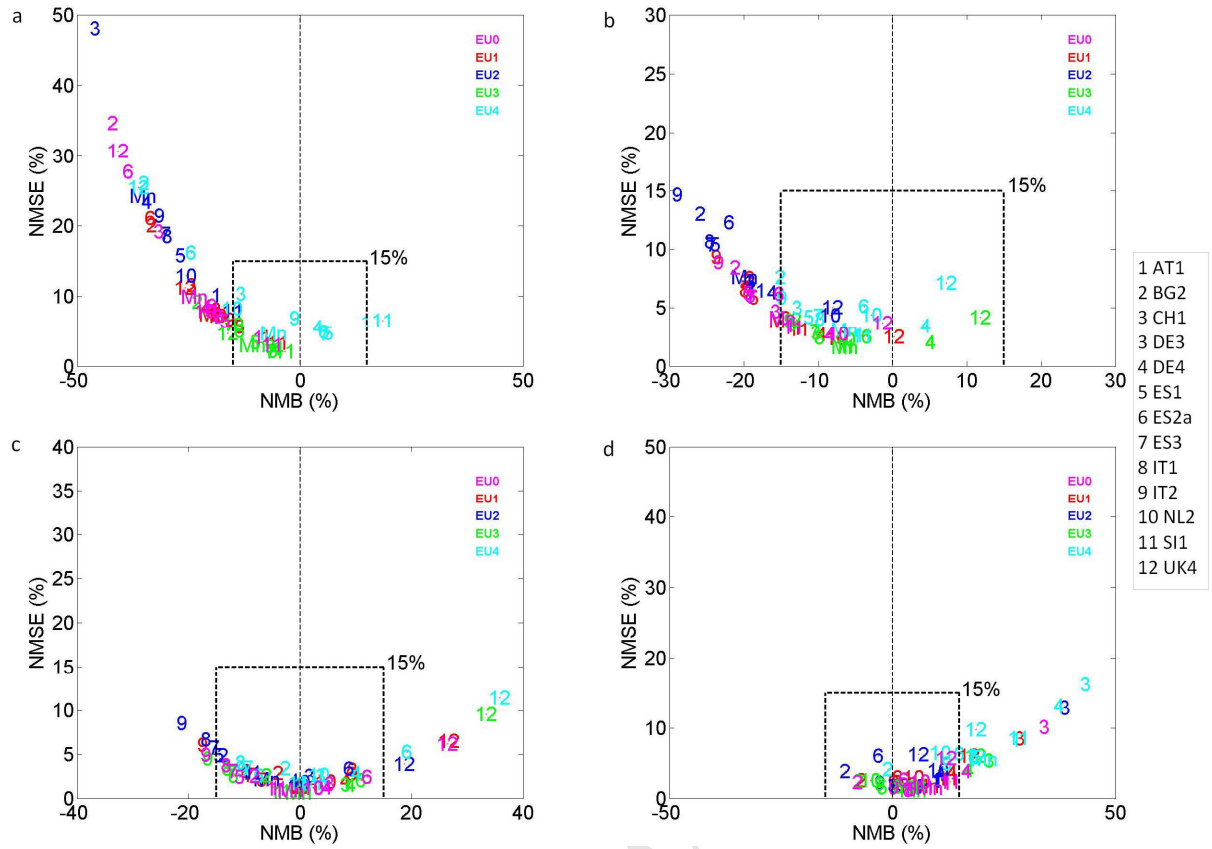


Fig.5.

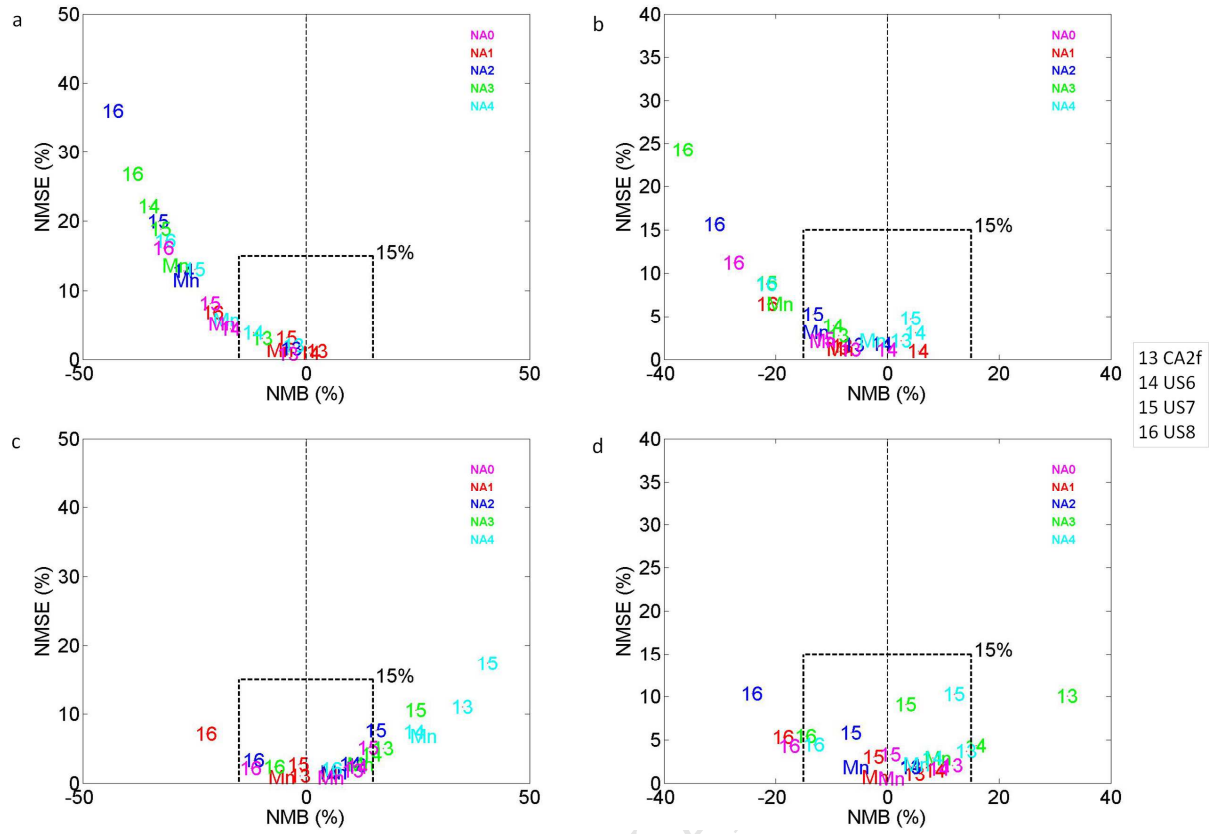


Fig.6.

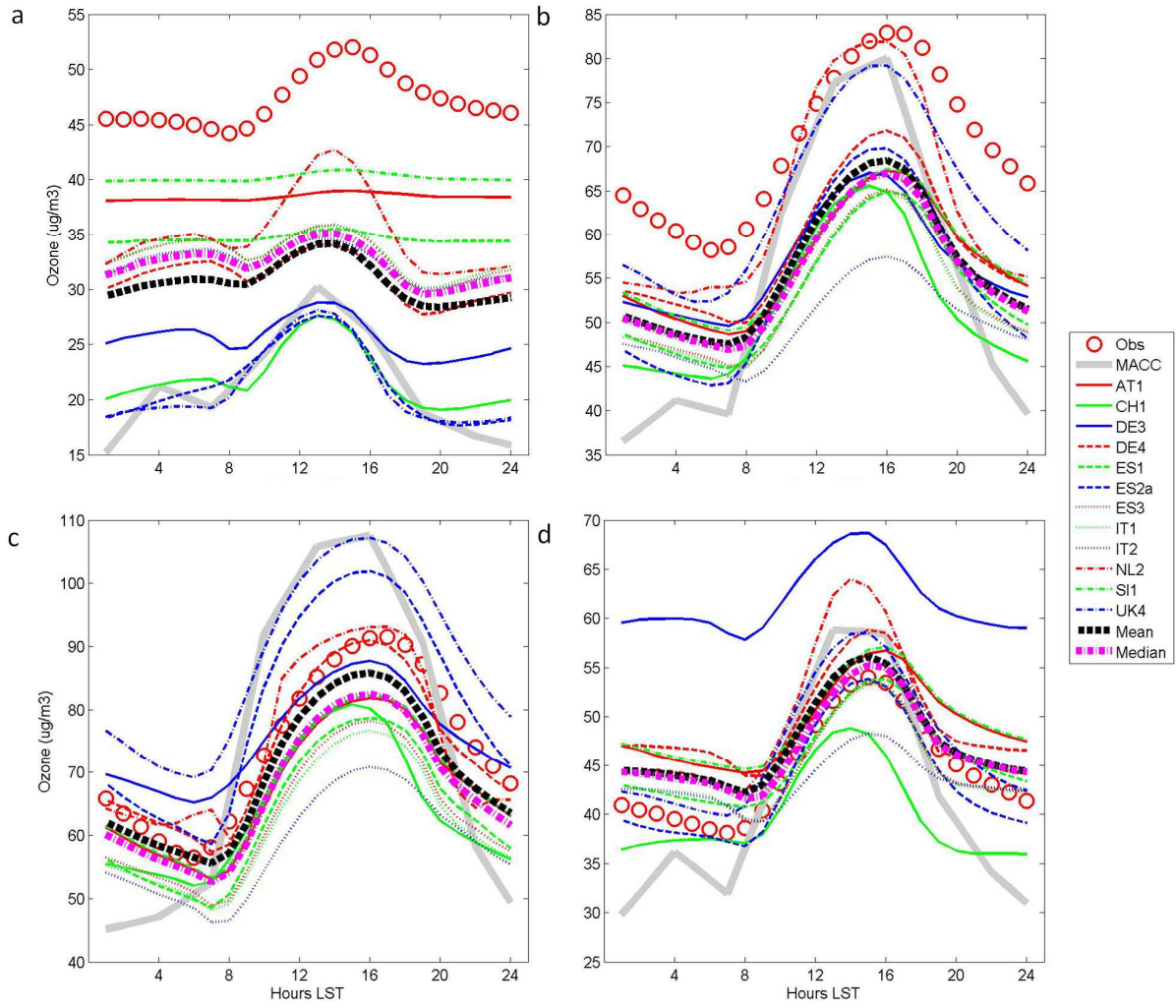


Fig.7.

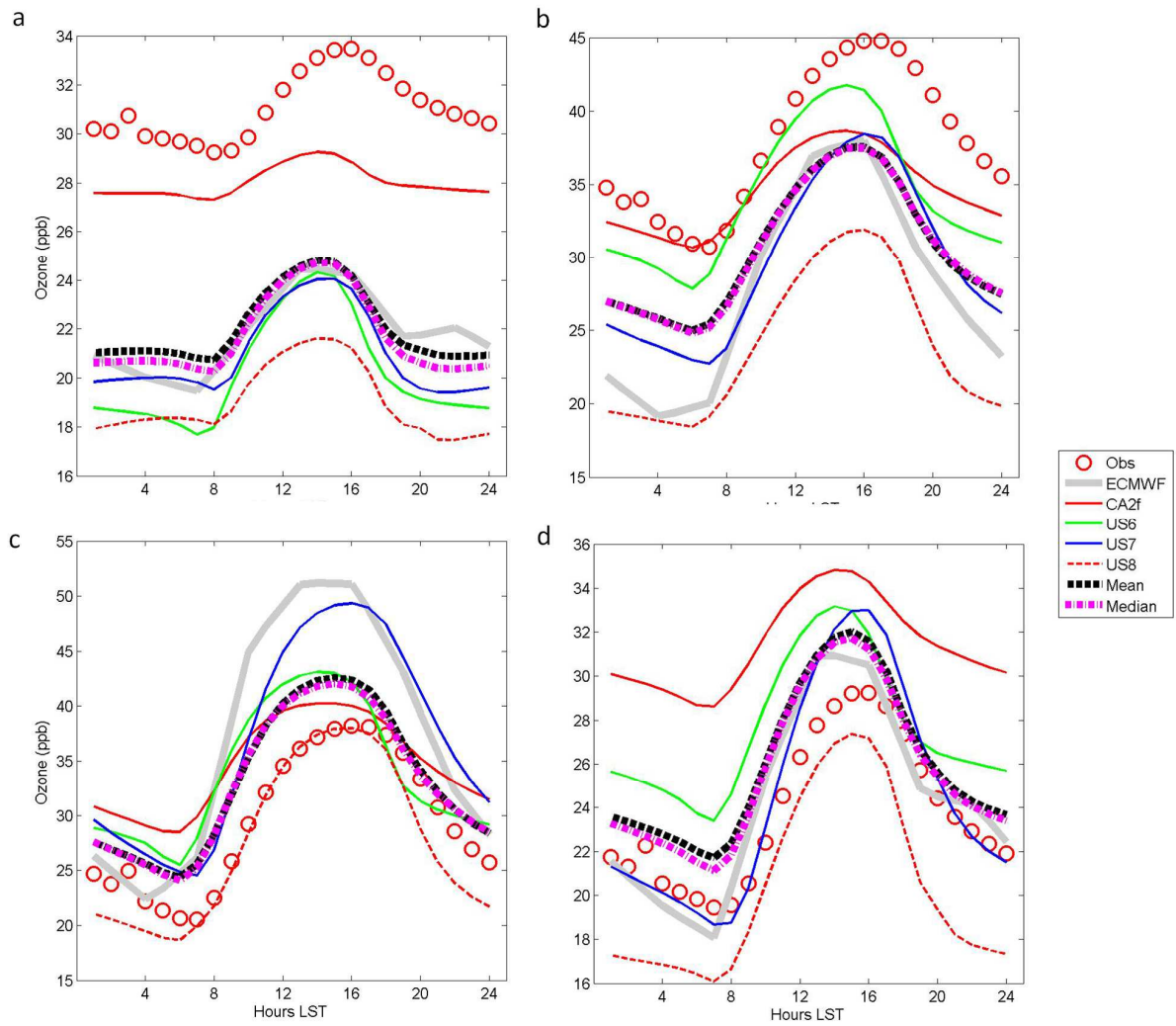


Fig.8.

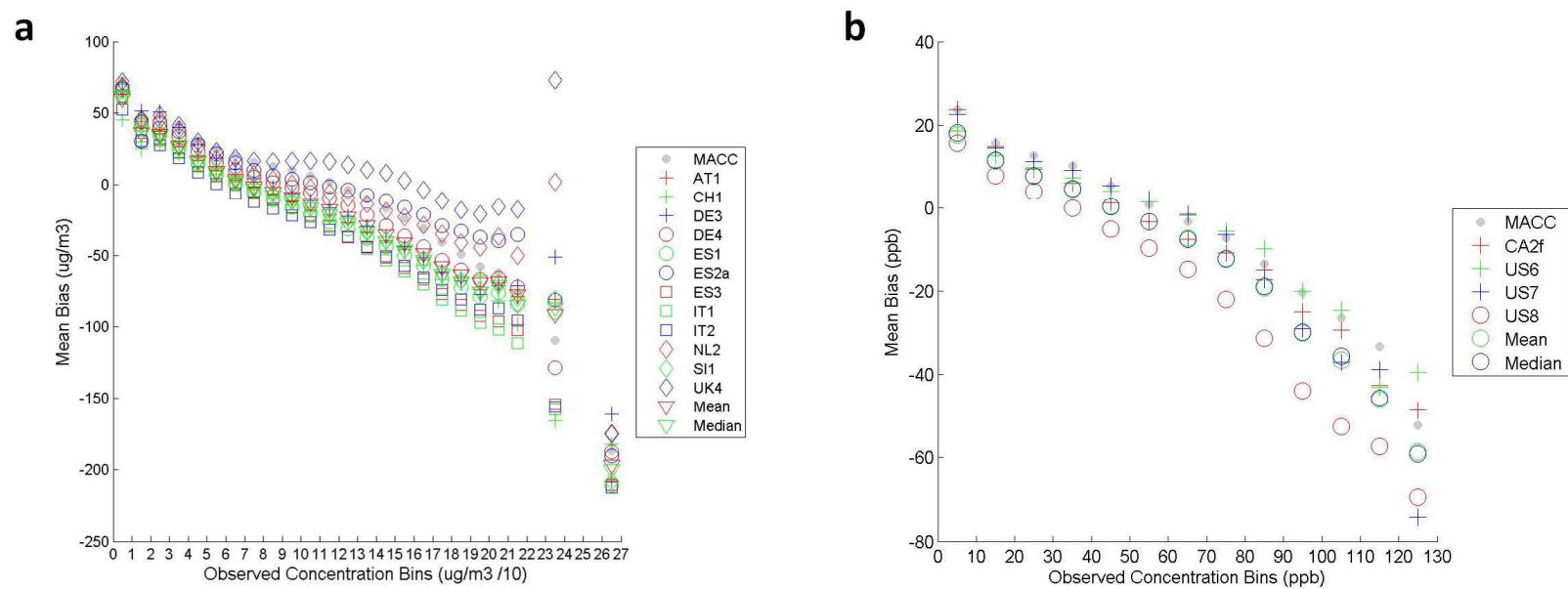


Fig.9.

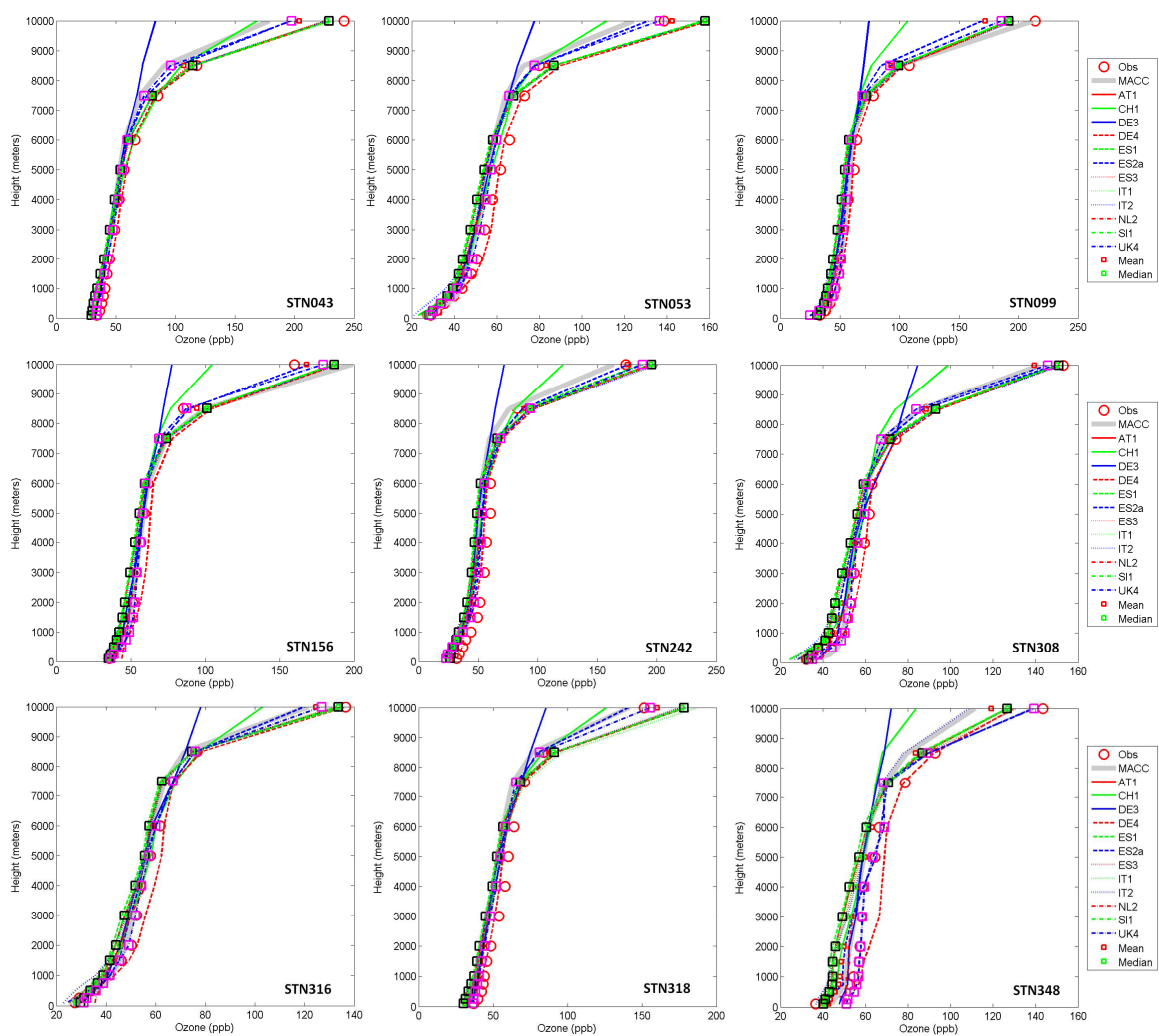


Fig.10.

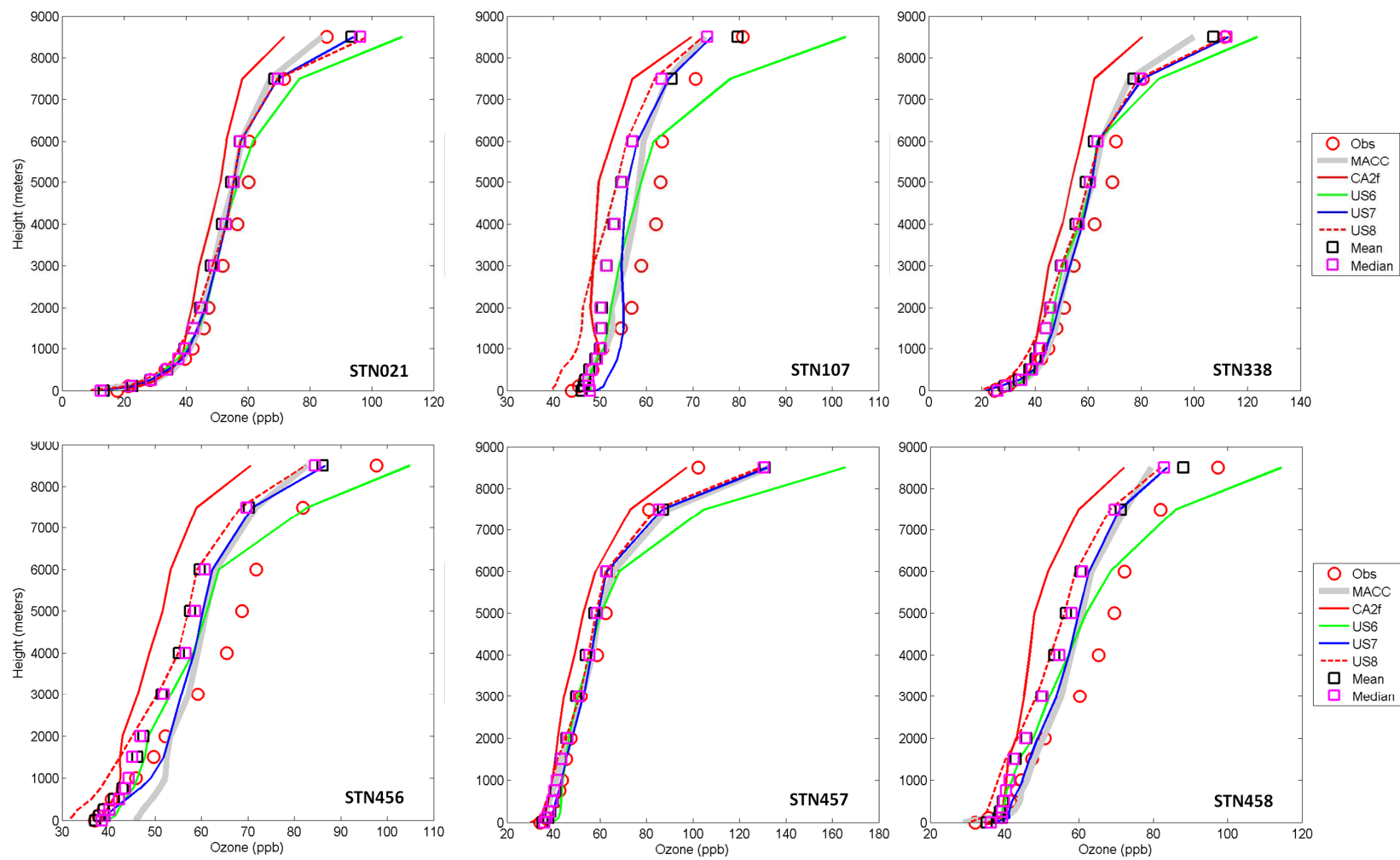


Fig.11.